

Computations of Quandle Cocycle Invariants of Knotted Curves and Surfaces

J. Scott Carter
University of South Alabama
Mobile, AL 36688
carter@mathstat.usouthal.edu

Daniel Jelsovsky
University of South Florida
Tampa, FL 33620
jelsovsk@math.usf.edu

Seiichi Kamada
Osaka City University
Osaka 558-8585, JAPAN
kamada@sci.osaka-cu.ac.jp

Masahico Saito
University of South Florida
Tampa, FL 33620
saito@math.usf.edu

August 20, 2018

Abstract

State-sum invariants for knotted curves and surfaces using quandle cohomology were introduced by Laurel Langford and the authors in [4]. In this paper we present methods to compute the invariants and sample computations. Computer calculations of cohomological dimensions for some quandles are presented. For classical knots, Burau representations together with MAPLE programs are used to evaluate the invariants for knot table. For knotted surfaces in 4-space, movie methods and surface braid theory are used. Relations between the invariants and symmetries of knots are discussed.

MRCN : Primary 57M25, 57Q45; Secondary 55N99, 18G99.

Keywords : Knots, knotted surfaces, quandle cohomology, state-sum invariants.

1 Introduction

In [4], we (with Laurel Langford) defined a state-sum invariant of classical links and of knotted orientable surfaces. The invariant uses the cohomology theory of racks and quandles developed in [14, 15, 16, 19] as its input. We modified the cohomology theory slightly to allow for type I Reidemeister moves and their higher dimensional analogues. Relations to linking numbers were given for some cocycles, and it was shown that an invariant can detect non-invertibility of the 2-twist spun trefoil [40, 42]. The nature of these invariants, however, is still a mystery.

The purpose of this paper is to present computational methods in a variety of contexts. The computational results have topological implications, such as non-invertibility for some knotted surfaces. For classical knots we use Burau representations of the braid group and finite quotients of the Alexander quandles to give computations. For small quandles these are well suited to desktop computer calculations. In the case of knotted surfaces in \mathbf{R}^4 we develop methods of computations using the theories of surface braids and movies. Our results are a combination of the above mentioned theories and computer calculations. The latter are supported by MAPLE and MATHEMATICA. Here we have concentrated on several important families of knots and knotted surfaces. In the classical case, we have computed several invariants in the knot table up to 9 crossings and torus knots. In the knotted surface case we have calculated for twist-spun torus knots (where the movies and surface braids follow some patterns), and for the movie of a deform-spun figure-8 knot. There are advantages to both the movie and the surface braid methods.

1.1 Organization. In Section 2 the basic definitions are reviewed from [4]. Section 3 presents cohomological dimensions for some Alexander quandles, after reviewing other calculations. Using some of these cocycles, invariants for knots in the table are computed in Section 4. Another good family of classical knots is torus knots. We prove some periodicity and computations of invariants for torus knots in Section 5. In Section 6, we give an explicit computation for a deform-spun figure-8 knot. This knotted sphere has 6 critical points, 16 triple points and no branch points. For twist spun torus knots in dimension 4, we use movie methods (Section 7) and surface braid theory (Section 8). Relations between the invariant and symmetries of knots are discussed in Section 9.

1.2 Acknowledgements. José Barrionuevo, Edwin Clark, and Cornelius Pillen had helpful programming hints for the computation of quandle cocycles. Seiichi Kamada is being supported by a Fellowship from the Japan Society for the Promotion of Science.

2 Definitions of Quandle Cocycle Invariants

2.1 Definition. A *quandle*, X , is a set with a binary operation $(a, b) \mapsto a * b$ such that

- (I) For any $a \in X$, $a * a = a$.
- (II) For any $a, b \in X$, there is a unique $c \in X$ such that $a = c * b$.
- (III) For any $a, b, c \in X$, we have $(a * b) * c = (a * c) * (b * c)$.

A *rack* is a set with a binary operation that satisfies (II) and (III). A typical example of a quandle is a group $X = G$ with n -fold conjugation as the quandle operation: $a * b = b^{-n}ab^n$. Racks and quandles have been studied in, for example, [3],[13],[23],[27], and [32]. The axioms for a quandle

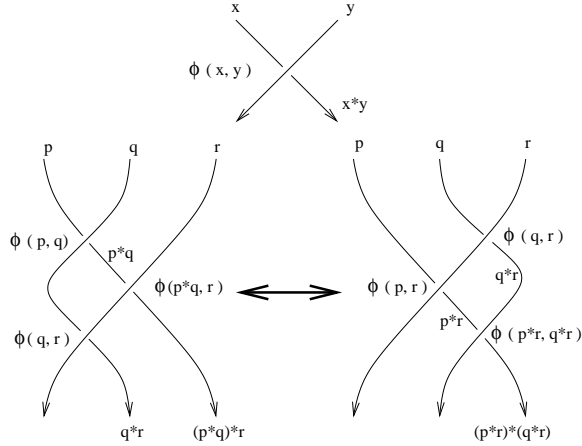


Figure 1: The 2-cocycle condition and the Reidemeister type III move

correspond respectively to the Reidemeister moves of type I, II, and III. (see also [13],[27]). Indeed, knot diagrams were one of the motivations to define such an algebraic structure.

2.2 Definition. Let X be a rack, and let A be an abelian group, written additively. The cochain group $C^n = C^n(X; A)$ is the abelian group of functions $f : \text{FA}(X^n) \rightarrow A$ from the free abelian group generated by n -tuples of elements from X to the abelian group A . The *coboundary homomorphism* $\delta : C^n \rightarrow C^{n+1}$ is defined by

$$\begin{aligned}
 (\delta f)(x_0, \dots, x_n) &= \sum_{i=1}^n (-1)^{i-1} f(x_0, \dots, \hat{x}_i, \dots, x_n) \\
 &+ \sum_{j=1}^n (-1)^j f(x_0 * x_j, \dots, x_{j-1} * x_j, x_{j+1}, \dots, x_n).
 \end{aligned}$$

(Note: Neither sum includes a 0th term as these terms cancel.)

The rest of the section is a review from [4].

2.3 Lemma. *The cochain group and the boundary homomorphism form a cochain complex.*

Proof. It is a routine calculation (that depends on axiom III of the rack) to check that $\delta \circ \delta = 0$. \square

2.4 Definition. The cohomology groups of the above complex are called *the rack cohomology groups* and are denoted by $H_{\text{rack}}^n(X, A)$. Also, the groups of cocycles and coboundaries are denoted by $Z_{\text{rack}}^n(X, A)$ and $B_{\text{rack}}^n(X, A)$ respectively. Their elements are called *n-cocycles* and *n-coboundaries*, respectively. This definition coincides with the cohomology theory defined in [14] and [15].

For applications, we are interested in the case when X is a quandle, so we will intersect the cocycles and coboundaries with a subset that captures axiom (I) and its consequences in higher dimensions. Let $P^n = \{f \in C^n : f(\vec{x}) = 0 \text{ for all } \vec{x} \text{ such that } x_j = x_{j+1} \text{ for some } j\}$. Let

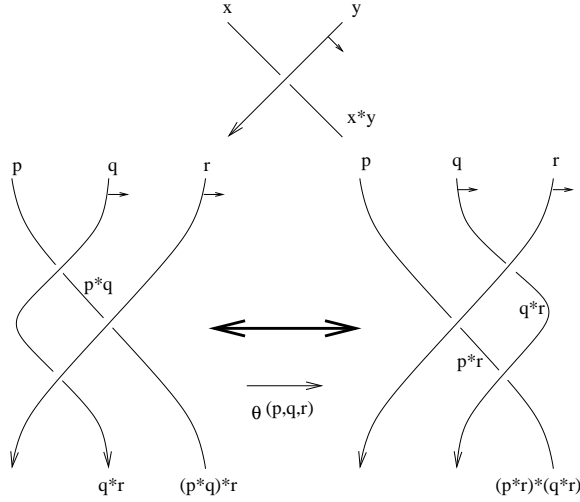


Figure 2: Assigning a 3-cocycle to a type III move (triple point)

$Z^n = Z_{\text{rack}}^n \cap P^n$, and $B^n = B_{\text{rack}}^n \cap P^n$. A straightforward calculation gives: if $f \in P^n$, then $\delta f \in P^{n+1}$ if X is a quandle. Define

$$H_Q^n(X, A) = H^n(X, A) = (P^n \cap Z_{\text{rack}}^n) / (P^n \cap B_{\text{rack}}^n).$$

This group is called the *quandle cohomology group*. The elements $f \in Z^n(X, A)$ are called *quandle n -cocycles* or simply *n -cocycles*.

Figures 1, 2, 3, and 4 indicate the relation between the cocycle conditions and the moves to classical knots and knotted surfaces. In Fig. 1, 2-cocycles are assigned to crossings. Then the type III Reidemeister move corresponds to the 2-cocycle condition. For knotted surfaces, 3-cocycles are assigned to triple points on projections, which are the type III Reidemeister moves in a movie description. Figure 2 shows the assignment of a 3-cocycle to a type III move. Figures 3 and 4 are movie descriptions of one of the generalized Reidemeister moves, called Roseman moves, which corresponds to the 3-cocycle condition.

2.5 Definition. A *color* (or *coloring*) on an oriented classical knot diagram is a function $\mathcal{C} : R \rightarrow X$, where X is a fixed quandle and R is the set of over-arcs in the diagram, satisfying the condition depicted in the top of Fig. 2. In the figure, a crossing with over-arc, r , has color $\mathcal{C}(r) = y \in X$. The under-arcs are called r_1 and r_2 from top to bottom; they are colored $\mathcal{C}(r_1) = x$ and $\mathcal{C}(r_2) = x * y$. If the pair of the co-orientation of the over-arc and that of the under-arc matches the (right-hand) orientation of the plane, then the crossing is called *positive*; otherwise it is *negative*. Note that locally the colors do not depend on the orientation of the under-arc.

Throughout this paper we consider only finite quandles.

2.6 Definition. Assume that a finite quandle X is given. Pick a quandle 2-cocycle $\phi \in Z^2(X, A)$, and write the coefficient group, A , multiplicatively. Consider a crossing in the diagram. For each

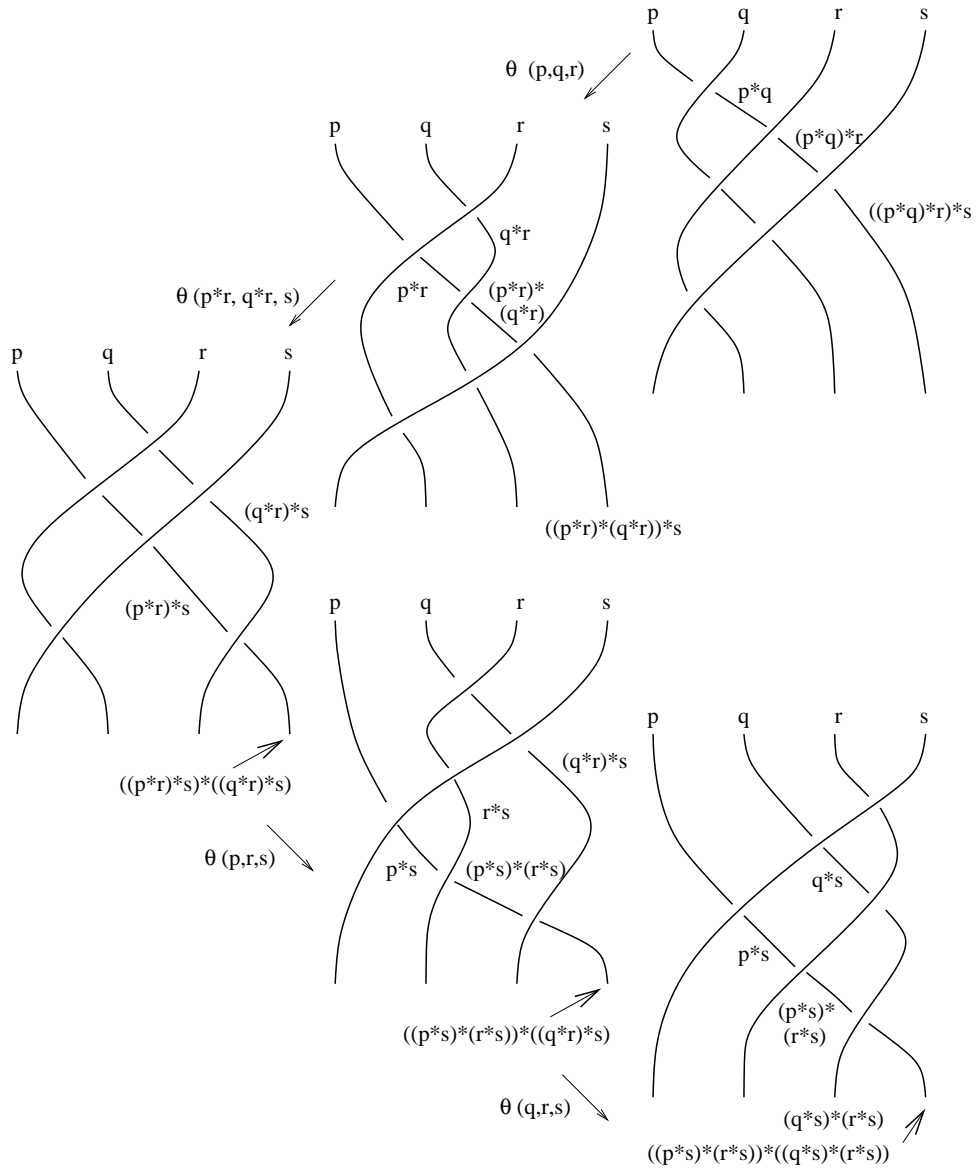


Figure 3: The tetrahedral move and a cocycle relation, LHS

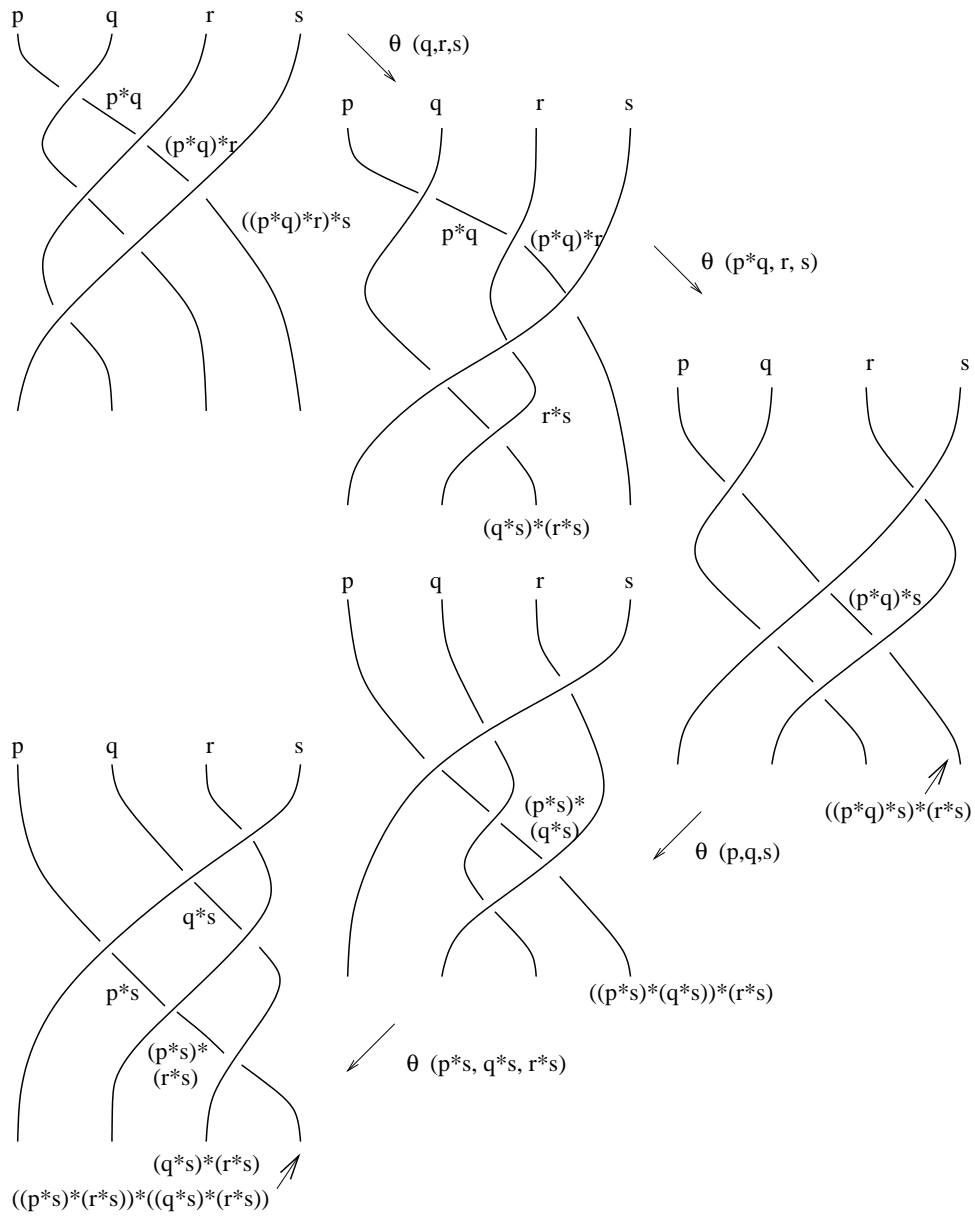


Figure 4: The tetrahedral move and a cocycle relation, RHS

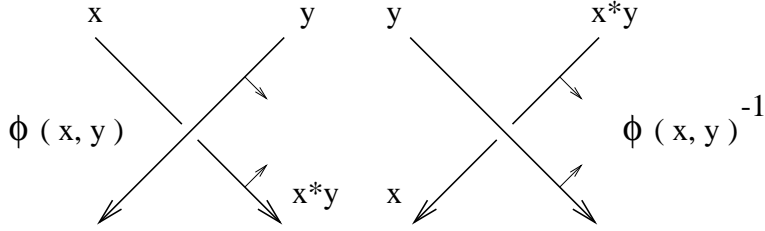


Figure 5: Weights for positive and negative crossings

coloring of the diagram, evaluate the 2-cocycle on two of the three quandle colors that appear near the crossing. One such color is the color on the upper arc and is the second argument of the 2-cocycle. The other color is the color on the under-arc away from which the normal arrow points; this is the first argument of the cocycle.

In Fig. 5, the two possible oriented and co-oriented crossings are depicted. The left is a positive crossing, and the right is negative. Let τ denote a crossing, and \mathcal{C} denote a coloring. When the colors of the segments are as indicated, the (Boltzmann) weights of the crossing, $B(\tau, \mathcal{C}) = \phi(x, y)^{\epsilon(\tau)}$, are as shown. These weights are assignments of cocycle values to the colored crossings where the arguments are as defined in the previous paragraph.

The *partition function*, or a *state-sum*, is the expression

$$\sum_{\mathcal{C}} \prod_{\tau} B(\tau, \mathcal{C}).$$

The product is taken over all crossings of the given diagram, and the sum is taken over all possible colorings. The values of the partition function are taken to be in the group ring $\mathbf{Z}[A]$ where A is the coefficient group.

2.7 Theorem. *The partition function is invariant under Reidemeister moves, so that it defines an invariant of knots and links. Thus it will be denoted by $\Phi(K)$ (or $\Phi_{\phi}(K)$ to specify the 2-cocycle ϕ used).*

With regard to the partition function, we easily obtain the following result.

2.8 Proposition. *If Φ_{ϕ} and $\Phi_{\phi'}$ denote the state-sum invariants defined from cohomologous cocycles ϕ and ϕ' then $\Phi_{\phi} = \Phi_{\phi'}$ (so that $\Phi_{\phi}(K) = \Phi_{\phi'}(K)$ for any link K). In particular, the state-sum is equal to the number of colorings of a given knot diagram if the 2-cocycle used for the Boltzmann weight is a coboundary.*

Before we define a similar invariant for knotted surfaces, we recall the notion of knotted surface diagrams. See [7] for details and examples. Let $f : F \rightarrow \mathbf{R}^4$ denote a smooth embedding of a closed surface F into 4-dimensional space. By deforming the map f slightly by an ambient isotopy in \mathbf{R}^4 if necessary, we may assume that $p \circ f$ is a general position map, where $p : \mathbf{R}^4 \rightarrow \mathbf{R}^3$ denotes the orthogonal projection onto an affine subspace.

Along the double curves, one of the sheets (called the *over-sheet*) lies farther than the other (*under-sheet*) with respect to the projection direction. The *under-sheets* are coherently broken in the projection, and such broken surfaces are called *knotted surface diagrams*.

When the surface is oriented, we take normal vectors \vec{n} to the projection of the surface such that the triple $(\vec{v}_1, \vec{v}_2, \vec{n})$ matches the right-handed orientation of 3-space, where (\vec{v}_1, \vec{v}_2) defines the orientation of the surface. Such normal vectors are defined on the projection at all points other than the isolated branch points.

2.9 Definition. A *color* on an oriented (broken) knotted surface diagram is a function $\mathcal{C} : R \rightarrow X$, where X is a fixed finite quandle and where R is the set of regions in the broken surface diagram, satisfying the following condition at the double point set.

At a double point curve, two coordinate planes intersect locally. One is the over-sheet r , the other is the under-sheet, and the under-sheet is broken into two components, say r_1 and r_2 . A normal of the over-sheet r points to one of the components, say r_2 . If $\mathcal{C}(r_1) = x \in X$, $\mathcal{C}(r) = y$, then we require that $\mathcal{C}(r_2) = x * y$.

2.10 Lemma. *The above condition is compatible at each triple point.*

Proof. The meaning of this lemma is as follows. There are 6 double curves near a triple point, giving 6 conditions on colors assigned. It can be checked in a straightforward manner that these conditions do not contradict each other. In particular, there is one of the 4 pieces of the lower sheet that receives color $(a * b) * c$ or $(a * c) * (b * c)$ depending on what path was followed to compute the color. Since these values agree in the quandle, there is no contradiction. \square

2.11 Definition. Note that when three sheets form a triple point, they have relative positions *top*, *middle*, *bottom* with respect to the projection direction of $p : \mathbf{R}^4 \rightarrow \mathbf{R}^3$. The *sign of a triple point* is positive if the normals of top, middle, bottom sheets in this order match the right-handed orientation of the 3-space. Otherwise the sign is negative.

2.12 Definition. A (Boltzmann) weight at a triple point, τ , is defined as follows. Let R be the octant from which all normal vectors of the three sheets point outwards; let a coloring \mathcal{C} be given. Let p, q, r be colors of the bottom, middle, and top sheets respectively, that bound the region R . Let $\epsilon(\tau)$ be the sign of the triple point, and θ be a quandle 3-cocycle. Then the Boltzmann weight $B(\tau, \mathcal{C})$ assigned to τ with respect to \mathcal{C} is defined to be $\theta(p, q, r)^{\epsilon(\tau)}$ where p, q, r are colors described above.

2.13 Definition. The *partition function*, or a *state-sum*, is the expression

$$\sum_{\mathcal{C}} \prod_{\tau} B(\tau, \mathcal{C})$$

where $B(\tau, \mathcal{C})$ is the Boltzmann weight assigned to τ . As in the classical case, we take the coefficient of the cohomology to be the group ring $\mathbf{Z}[A]$ where A is the coefficient group written multiplicatively.

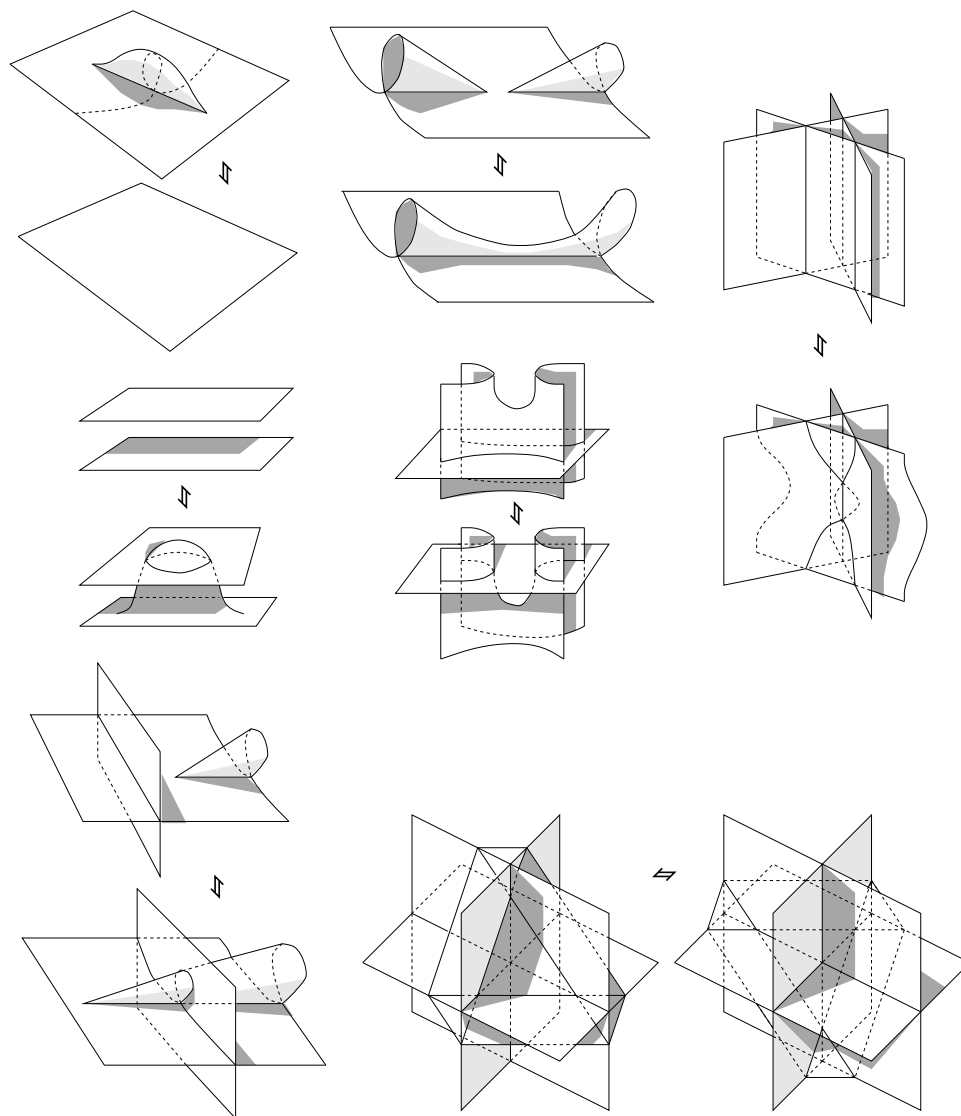


Figure 6: Roseman moves for knotted surface diagrams

2.14 Theorem. *The partition function does not depend on the choice of knotted surface diagram. Thus it is an invariant of knotted surfaces F , and denoted by $\Phi(F)$ (or $\Phi_\theta(F)$ to specify the 3-cocycle θ used).*

Proof Sketch. Roseman generalized Reidemeister moves to knotted surfaces, and their projections are depicted in Fig. 6 [7, 37]. Thus two knotted surface diagrams represent isotopic knotted surface if and only if the diagrams are related by a finite sequence of moves, called *Roseman moves*, taken from this list. The well-definedness of the state-sum is proved by showing that it remains invariant under the Roseman moves. In particular, Figs. 3 and 4 represent movie descriptions of the tetrahedral move, which involves four general position planes (right-bottom of Fig. 6). Thus these figures show that the state-sum is invariant under this move, for a specific choice of orientations. Other cases are checked to prove the well-definedness. \square

As in the classical dimension, we can show the following.

2.15 Proposition. *If Φ_θ and $\Phi_{\theta'}$ denote the state-sum invariants defined from cohomologous cocycles θ and θ' then $\Phi_\theta = \Phi_{\theta'}$ (so that $\Phi_\theta(K) = \Phi_{\theta'}(K)$ for any knotted surface K). In particular, if θ is a 3-coboundary, then the state-sum defined above is equal to the number of colorings.*

3 Non-trivial Cocycles

Here we define a few exemplary quandles and give some quandle cocycles that are not coboundaries.

3.1 Presentation of the Cohomology Groups. Suppose that the coefficient group A is either a cyclic group, \mathbf{Z} , \mathbf{Z}_n , or the rational numbers, \mathbf{Q} . Define a *characteristic function*

$$\chi_x(y) = \begin{cases} 1 & \text{if } x = y \\ 0 & \text{if } x \neq y \end{cases}$$

from the free abelian group generated by X^n to the group A . The set $\{\chi_x : x \in X^n\}$ of such functions spans the group $C_{\text{rack}}^n(X, A)$ of cochains. Thus if $f \in C_{\text{rack}}^n(X, A)$ is a cochain, then

$$f = \sum_{x \in X^n} C_x \chi_x.$$

We are interested in those f s in P^n ; *i.e.* those homomorphisms that vanish on $S = \{(x_1, \dots, x_n) \in X^n : x_j = x_{j+1} \text{ for some } j\}$. So we can write

$$f = \sum_{x \in X^n \setminus S} C_x \chi_x.$$

If $\delta f = 0$, then f vanishes on expressions of the form

$$\sum_j (-1)^{j+1} (x_0, \dots, \hat{x}_j, \dots, x_n) + \sum_k (-1)^k (x_0 * x_k, \dots, x_{k-1} * x_k, x_{k+1}, \dots, x_n).$$

In computing the cohomology we consider all such expressions as (x_0, \dots, x_n) ranges over all $(n+1)$ -tuples for which each consecutive pair of elements is distinct. By evaluating linear combinations of characteristic functions on these expressions, we determine those functions that are cocycles. Similarly, we compute the coboundary on each of the characteristic functions in the previous dimension, to determine which linear combinations of characteristic functions are coboundaries.

3.2 Definition [13]. A rack is called *trivial* if $x * y = x$ for any x, y .

The *dihedral quandle* R_n of order n is the quandle consisting of reflections of the regular n -gon with the conjugation as operation. The dihedral group D_{2n} has a presentation

$$\langle x, y | x^2 = 1 = y^n, xyx = y^{-1} \rangle$$

where x is a reflection and y is a rotation of a regular n -gon. The set of reflections R_n in this presentation is $\{a_i = xy^i : i = 0, \dots, n-1\}$ where we use the subscripts from \mathbf{Z}_n in the following computations. The operation is

$$a_i * a_j = a_j^{-1} a_i a_j = xy^j xy^i xy^j = xy^j y^{-i} y^j = a_{2j-i}.$$

Compare with the well known n -coloring of knot diagrams [17].

The quandles with three elements are classified in [13] and consist of three isomorphic classes, the trivial one, R_3 , and P_3 .

Let S_4 denote the quandle with four elements, denoted by 0, 1, 2, 3, with the relations

$$\begin{aligned} 0 &= 0 * 0 = 1 * 2 = 2 * 3 = 3 * 1 \\ 1 &= 0 * 3 = 1 * 1 = 2 * 0 = 3 * 2 \\ 2 &= 0 * 1 = 1 * 3 = 2 * 2 = 3 * 0 \\ 3 &= 0 * 2 = 1 * 0 = 2 * 1 = 3 * 3. \end{aligned}$$

This quandle is the following set of 3-cycles in the permutation group on 4 elements: $\{0 = (243), 1 = (134), 2 = (142), 3 = (123)\}$ with conjugation as the operation.

3.3 Lemma. *Any cochain on a trivial quandle is a cocycle. Only the zero map is a coboundary.*

Proof. This follows from the definitions. \square

In [4, 14, 15, 16, 19], cohomology groups are computed for some quandles. A MAPLE program is found in [21]. The techniques that we used in [4] are applied to give the following:

- $H_Q^2(R_3, A) = 0$ for any A ,
- $H_Q^2(R_4, \mathbf{Z}_2) = (\mathbf{Z}_2)^4$,
- $H_Q^2(R_4, A) = A \times A$ for any A without order 2 elements,
- $H_Q^2(R_5, A) = 0$ for any A ,
- $H_Q^2(R_6, A) = A \times A$ for any A ,
- $H_Q^2(S_4, \mathbf{Z}_2) = \mathbf{Z}_2$,
- $H_Q^2(S_4, A) = 0$ for any A without order 2 elements

For the third cohomology, we have

- $H_Q^3(P_3, A) = A \times A$ for any A ,

- $H_Q^3(R_3, \mathbf{Z}_3) = \mathbf{Z}_3$,
- $H_Q^3(R_3, A) = 0$ for any A without order 3 elements,
- $H_Q^3(R_4, \mathbf{Z}_2) = (\mathbf{Z}_2)^8$,
- $H_Q^3(R_4, \mathbf{Z}_q) = \mathbf{Z}_q \times \mathbf{Z}_q$ for any odd prime q ,
- $H_Q^3(R_4, \mathbf{Z}) = \mathbf{Z} \times \mathbf{Z} \times \mathbf{Z}_2 \times \mathbf{Z}_2$,
- $H_Q^3(R_4, \mathbf{Q}) = \mathbf{Q} \times \mathbf{Q}$,
- $H_Q^3(R_5, \mathbf{Z}_5) = \mathbf{Z}_5$,
- $H_Q^3(R_5, A) = 0$ for any A without order 5 elements,
- $H_Q^3(S_4, \mathbf{Z}_2) = (\mathbf{Z}_2)^3$,
- $H_Q^3(S_4, \mathbf{Z}_4) = (\mathbf{Z}_2)^2 \times \mathbf{Z}_4$,
- $H_Q^3(S_4, \mathbf{Z}_q) = 0$ for any odd prime q ,
- $H_Q^3(S_4, \mathbf{Z}) = \mathbf{Z}_2$,
- $H_Q^3(S_4, \mathbf{Q}) = 0$.

An important class of quandles are Alexander quandles.

3.4 Definition [13, 27]. Let $\Lambda = \mathbf{Z}[T, T^{-1}]$ be the Laurent polynomial ring over the integers. Then any Λ -module M has a quandle structure defined by $a * b = Ta + (1 - T)b$ for $a, b \in M$.

There are many Λ -modules such that $L \otimes_{\mathbf{Z}} \mathbf{Z}_n$ is a finite quandle. When $\mathbf{Z}_n[T, T^{-1}]/(h(T))$ is a finite quandle, it is called a *(mod n)-Alexander quandles*. Let us point out an exceptional case. Suppose that $\gcd(a, n) > 1$, and consider $\Lambda_{n,a} = \mathbf{Z}_n[T, T^{-1}]/(T - a)$. Then $\Lambda_{n,a}$ is not a quandle because axiom II fails. If $\gcd(a, n) = 1$, then $\Lambda_{n,a}$ is a quandle.

Some of the quandles we have already seen are related to Alexander quandles.

- $\mathbf{Z}_n[T, T^{-1}]/(T + 1) \cong R_n$,
- $\mathbf{Z}_2[T, T^{-1}]/(T^2 - 1) \cong R_4$,
- $\mathbf{Z}_2[T, T^{-1}]/(T^2 + T + 1) \cong S_4$ (The correspondence is $0 \leftrightarrow 0$, $1 \leftrightarrow 1$, $2 \leftrightarrow 1 + T$, and $3 \leftrightarrow T$).

3.5 Table. Extending these results, we give the following table (next page) of cohomological dimensions for some quandles with mod p coefficients (where p is a prime), computed by MAPLE. The orders q of the coefficient groups $A = \mathbf{Z}_q$ are indicated in the table. The quandles are chosen as follows. First, the programs require time beyond our patience for quandles of larger than ten elements. Second, Burau matrices enable us to write a program to compute invariants for knots in the knot table (which will be presented in the next section) for Alexander quandles, and all examples of quandles we have dealt with are Alexander quandles (dihedral quandles are the case

$T = -1$ in the Alexander quandles). Hence, we computed for Alexander quandles of less than 10 elements, and we considered the Alexander quandles of the form $\mathbf{Z}_p[T, T^{-1}]/(h(T))$, where h is a polynomial whose leading and constant terms are invertible in \mathbf{Z}_p for the quandle to be finite. By multiplying by a unit, we can assume that such polynomials are monic. In the case $\deg(h(T)) = 3$, typical elements are of the form $a + bT + cT^2$ and hence the quandle has the order p^3 , and for this order to be less than 10, we only have the choice $p = 2$, and the choices of $h(T)$ are $T^3 + 1$, $T^3 + T^2 + 1$, and $T^3 + T + 1$ that are listed in the table below as the last 3 entrees. The cases for smaller degrees are as shown in the table.

quandle Q	order	$q = \setminus \dim H^2(Q, \mathbf{Z}_q)$								$\dim H^3(Q, \mathbf{Z}_q)$				
		2	3	5	7	11	13	17	19	2	3	5	7	11
R_3	3	0	0	0	0	0	0	0	0	0	1	0	0	0
R_4	4	4	2	2	2	2	2	2	2	8	2	2	2	2
R_5	5	0	0	0	0	0	0	0	0	0	0	1	0	0
R_6	6	2	2	2	2	2	2	2	2	2	4	2	2	2
R_7	7	0	0	0	0	0	0	0	0					
R_8	8	4	2	2	2	2	2	2	2					
R_9	9	0	0	0	0	0	0	0	0					
$\mathbf{Z}_5[T, T^{-1}]/(T - 2)$	5	0	0	0	0	0	0	0	0	0	0	0	0	0
$\mathbf{Z}_5[T, T^{-1}]/(T - 3)$	5	0	0	0	0	0	0	0	0	0	0	0	0	0
$\mathbf{Z}_7[T, T^{-1}]/(T - 2)$	7	0	0	0	0	0	0	0	0					
$\mathbf{Z}_7[T, T^{-1}]/(T - 3)$	7	0	0	0	0	0	0	0	0					
$\mathbf{Z}_7[T, T^{-1}]/(T - 4)$	7	0	0	0	0	0	0	0	0					
$\mathbf{Z}_7[T, T^{-1}]/(T - 5)$	7	0	0	0	0	0	0	0	0					
$\mathbf{Z}_8[T, T^{-1}]/(T - 3)$	8	4	2	2	2	2	2	2	2					
$\mathbf{Z}_8[T, T^{-1}]/(T - 5)$	8	16	12	12	12	12	12	12	12					
$\mathbf{Z}_9[T, T^{-1}]/(T - 2)$	9	0	0	0	0	0	0	0	0					
$\mathbf{Z}_9[T, T^{-1}]/(T - 4)$	9	6	9	6	6	6	6	6	6					
$\mathbf{Z}_9[T, T^{-1}]/(T - 5)$	9	0	0	0	0	0	0	0	0					
$\mathbf{Z}_2[T, T^{-1}]/(T^2 + 1)$	4	2	0	0	0	0	0	0	0	8	2	2	2	2
$\mathbf{Z}_2[T, T^{-1}]/(T^2 + T + 1)$	4	1	0	0	0	0	0	0	0	3	0	0	0	0
$\mathbf{Z}_3[T, T^{-1}]/(T^2 + 1)$	9	0	1	0	0	0	0	0	0					
$\mathbf{Z}_3[T, T^{-1}]/(T^2 - 1)$	9	6	6	6	6	6	6	6	6					
$\mathbf{Z}_3[T, T^{-1}]/(T^2 + T + 1)$	9	3	6	3	3	3	3	3	3					
$\mathbf{Z}_3[T, T^{-1}]/(T^2 - T + 1)$	9	0	0	0	0	0	0	0	0					
$\mathbf{Z}_3[T, T^{-1}]/(T^2 + T - 1)$	9	0	0	0	0	0	0	0	0					
$\mathbf{Z}_2[T, T^{-1}]/(T^3 + 1)$	8	4	2	2	2	2	2	2	2					
$\mathbf{Z}_2[T, T^{-1}]/(T^3 + T^2 + 1)$	8	0	0	0	0	0	0	0	0					
$\mathbf{Z}_2[T, T^{-1}]/(T^3 + T + 1)$	8	0	0	0	0	0	0	0	0					

Table 3.5 : Cohomological dimensions of Alexander quandles

3.6 Remark. We conjecture that the dimension with $A = \mathbf{Z}$ is the dimension for prime q 's when they have the same value for most of them we computed. For example, we already know [4] that $H^2(R_4, \mathbf{Z}) = \mathbf{Z}^2$ and in Table 3.5 we have dimensions 2 for all q but $q = 2$. So it is natural to conjecture the same pattern for other quandles when it happens.

3.7 Remark. The blank entries in Table 3.5 means that MAPLE did not finish computations of the first item of the program within 24 hours.

3.8 Remark. In Table 3.5, $\mathbf{Z}_9[T, T^{-1}]/(T-7)$ is omitted since it is isomorphic to $\mathbf{Z}_9[T, T^{-1}]/(T-4)$; the mapping

$$f(0) = 0, f(1) = 1, f(2) = 2, f(3) = 6, f(4) = 7, f(5) = 8, f(6) = 3, f(7) = 4, f(8) = 5$$

gives an isomorphism.

Two quandles Q and R are said to be *dual quandles* if there is a one-to-one correspondence $\gamma : Q \rightarrow R$ between their elements, and $\gamma(a) * \gamma(b) = \gamma(a\bar{*}b)$ where $c = a\bar{*}b$ is the unique element $c \in Q$ such that $a = c*b$. In general, if $ab \equiv 1 \pmod{p}$, then $\mathbf{Z}_p[T, T^{-1}]/(T-a)$ and $\mathbf{Z}_p[T, T^{-1}]/(T-b)$ are dual quandles. The above quandles, $\mathbf{Z}_9[T, T^{-1}]/(T-4)$ and $\mathbf{Z}_9[T, T^{-1}]/(T-7)$, are not only isomorphic but also dual of each other. More generally, we have the following.

3.9 Lemma. *The quandles $\mathbf{Z}_p[T, T^{-1}]/(T-a)$ and $\mathbf{Z}_p[T, T^{-1}]/(T-b)$ are dual to each other if $ab \equiv 1 \pmod{p}$. (We assume $\gcd(p, a) = \gcd(p, b) = 1$ so that the quandles have p elements. In this case we denote $\mathbf{Z}_p[T, T^{-1}]/(T-a)$ by $\Lambda_{p,a}$.)*

Proof. Consider the identity map $\mathbf{Z}_p \rightarrow \mathbf{Z}_p$. $x *_1 y = ax + (1-a)y$ and $x *_2 y = bx + (1-b)y$. The dual of $\mathbf{Z}_p[T, T^{-1}]/(T-b)$ has the operation $x\bar{*}_2 y = (x + (b-1)y)b^{-1}$. However if $ab \equiv 1$ (hence $b^{-1} = a$), then $x\bar{*}_2 y = (x + (b-1)y)a = ax + (1-a)y = x *_1 y$. Hence $\Lambda_{p,a}$ is dual to $\Lambda_{p,b}$. \square

In a subsequent paper, we will prove that dual quandles have isomorphic cohomology groups.

3.10 Remark. Recall that $\Lambda_{9,4}$ and $\Lambda_{9,7}$ are isomorphic. This implies that $\Lambda_{9,4}$ is “self-dual”, *i.e.*, isomorphic to its dual. In general, $\Lambda_{p,a}$ is not self-dual, and hence $\Lambda_{p,a}$ is not isomorphic to $\Lambda_{p,b}$ even if $ab \equiv 1 \pmod{p}$.

We have that $\Lambda_{5,2}$ is not isomorphic to $\Lambda_{5,3}$, $\Lambda_{7,3}$ is not isomorphic to $\Lambda_{7,5}$.

3.11 Question. When are $\Lambda_{p,a}$ is isomorphic to $\Lambda_{p,b}$ with $ab \equiv 1 \pmod{p}$? Equivalently, when is $\Lambda_{p,a}$ self-dual?

4 Computations for Knot Table

For Alexander quandles, closed braids and Burau representations can be used to compute the cocycle invariants. In this section we present computational results obtained by MAPLE. The MAPLE program we used in this section can be found in [21]. Here is a sketch of an algorithm we used.

1. We used the same program that we used in the preceding section to compute cocycle groups for Alexander quandles. Then we made specific choices of cocycles. The choices are made after some experiments.
2. If $B = \begin{bmatrix} 0 & T \\ 1 & 1 - T \end{bmatrix}$ is the Burau matrix, and v is a row vector of Λ^2 , where Λ is an Alexander quandle, representing the colors assigned to the top two strings at a positive crossing, then the colors at the bottom strings are represented by a vector vB . Furthermore, the cocycle contribution at this crossing is $\phi(v_1, v_2)$ where $v = (v_1, v_2)$. The actual vectors have larger dimensions depending on the braid index of the given closed braid, but it is simply shifted to the position of the corresponding braid generator.
3. If $B(w)$ is the Burau representation of a braid word w , then a vector v colors the closed braid if and only if $vB(w) = v$. The MAPLE program searches for all such colors, and then evaluates the state-sum contributions.

We used the closed braid form for knots in the table given in [22] up to (including) 9 crossings to obtain the following results. We list some of the quandles with non-trivial cohomology computed in the preceding section. We chose q with highest dimensions among all non-zero dimensions. We conjecture that the invariants are positive integers for knots with R_n if n is even. Note that some quandles have non-trivial values for links [4], and could define interesting invariants for links even if they are trivial for knots.

1. For $\mathbf{Z}_2[T, T^{-1}]/(T^2 + 1)$ with the coefficient $A = \mathbf{Z}_2$ all knots in the table up to 9 crossings have the trivial invariant (have value 4). Thus none colors non-trivially.

For $\mathbf{Z}_9[T, T^{-1}]/(T - 4)$ and $\mathbf{Z}_3[T, T^{-1}]/(T^2 + T + 1)$ with $A = \mathbf{Z}_3$, all knots of the first half (42 out of 84) of the table up to 9 crossings have the trivial invariant (have value 9). We stopped the program after 5 days.

2. For $S_4 = \mathbf{Z}_2[T, T^{-1}]/(T^2 + T + 1)$ with the coefficient $A = \mathbf{Z}_2$, we used the cocycle $\phi = \prod \chi_{(a,b)}$ where the product is taken over all pairs (a, b) such that $a, b \in \{0, 1, T + 1\}$ and $a \neq b$. The invariants take the following values.

- $4(1 + 3t)$ for $3_1, 4_1, 7_2, 7_3, 8_1, 8_4, 8_{11}, 8_{13}, 9_1, 9_6, 9_{12}, 9_{13}, 9_{14}, 9_{21}, 9_{23}, 9_{35}, 9_{37}$.
- $16(1 + 3t)$ for $8_{18}, 9_{40}$.
- 16 for $8_5, 8_{10}, 8_{15}, 8_{19} - 8_{21}, 9_{16}, 9_{22}, 9_{24}, 9_{25}, 9_{28} - 9_{30}, 9_{36}, 9_{38}, 9_{39}, 9_{41} - 9_{45}, 9_{49}$.
- 4 otherwise.

3. For $\mathbf{Z}_3[T, T^{-1}]/(T^2 + 1)$ with the coefficient $A = \mathbf{Z}_3$, we used the cocycle

$$\begin{aligned}
\phi = & \chi_{2T, 2} + 2\chi_{2T, T} + 2\chi_{2T, 1+T} + 2\chi_{2T, 2+T} + 2\chi_{1+2T, 0} + 2\chi_{1+2T, 1} + 2\chi_{1+2T, 2} + \chi_{1+2T, T} \\
& + \chi_{1+2T, 1+T} + \chi_{1+2T, 2+T} + \chi_{2T, 1} + \chi_{2T, 0} + 2\chi_{0, 2T} + 2\chi_{0, 2+T} + \chi_{0, T} + \chi_{0, 2} \\
& + 2\chi_{0, 1} + 2\chi_{1, 2T} + \chi_{1, 2+T} + 2\chi_{1, 1+T} + 2\chi_{1, 2} + \chi_{1, 0} + \chi_{0, 1+2T} + \chi_{2, 1} \\
& + 2\chi_{2, 0} + \chi_{1, 1+2T} + \chi_{2, 1+2T} + 2\chi_{2, 2T} + \chi_{2, 1+T} + 2\chi_{2, T} + \chi_{T, 2} + 2\chi_{T, 0} \\
& + \chi_{T, 1+T} + 2\chi_{T, 2+T} + \chi_{T, 2T} + 2\chi_{T, 1+2T} + \chi_{1+T, 1} + 2\chi_{1+T, T} + 2\chi_{1+T, 2} + \chi_{1+T, 2+T} \\
& + 2\chi_{1+T, 1+2T} + \chi_{1+T, 2T} + \chi_{2+T, 0} + 2\chi_{2+T, 1+T} + \chi_{2+T, T} + \chi_{2+T, 2T} + 2\chi_{2+T, 1+2T}.
\end{aligned}$$

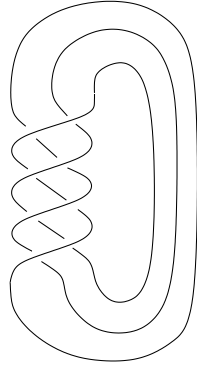


Figure 7: The torus knot $T(3,4)$

The invariants take the following values.

- $9(1 + 4t + 4t^2)$ for $4_1, 5_2, 8_3, 8_{17}, 8_{18}, 8_{21}, 9_6, 9_7, 9_{11}, 9_{24}, 9_{26}, 9_{37} - 9_{39}, 9_{47}$.
- $297 + 216t + 216t^2$ for 9_{40} .
- 81 for $6_3, 8_2, 8_{19}, 8_{24}, 9_{12}, 9_{13}, 9_{46}$.
- 9 otherwise.

4.1 Remark. With S_4 , we do not know any knot with the invariant not equal to an integer or $k(4 + 12t)$ for an integer k . However, the torus link $T(5,15)$ has the invariant $544 + 480t$ (with S_4 and $A = \mathbf{Z}_2$, with the same cocycle as above).

5 Computations for Torus Knots

The Burau matrices for torus knots have periodicities with some quandles. In this section we give such periodicities and use them to compute the invariants for torus knots. Throughout the section let Q be a finite Alexander quandle ($Q = \mathbf{Z}_m[T, T^{-1}]/(h(T))$ for some positive integer m and a Laurent polynomial $h(T)$).

Consider a (n, k) -torus knot or link $L = T(n, k)$ (Fig. 7 depicts $T(3, 4)$). Then L may be represented as the closure of an n -string braid β of the form $(\sigma_{n-1}\sigma_{n-2}\dots\sigma_1)^k$. If we color this braid by the quandle Q , any possible color of the closed braid $\hat{\beta}$ can be uniquely determined by a choice of colors on the top segment of the n -strands expressed as a vector, say $[a_1, a_2, \dots, a_n]$ where $a_i \in Q$ for $i = 1, 2, \dots, n$, which we call a color vector. Note that $[a_1, a_2, \dots, a_n] = \sum_{i=1}^n a_i e_i$, where e_i is a basic unit vector, with all 0 except a 1 in the i -th position.

The braid word $\sigma_{n-1}\sigma_{n-2}\dots\sigma_1$ on strands colored $[a_1, a_2, \dots, a_n]$ on the top ends alters this n -tuple of colors to the color vector $[a_n, a_1 * a_n, \dots, a_{n-1} * a_n]$ assigned on the strings below the word $\sigma_{n-1}\sigma_{n-2}\dots\sigma_1$. This operation can be represented by multiplying the color vector on the

right by the $n \times n$ matrix

$$A = \begin{bmatrix} 0 & T & \dots & 0 \\ \vdots & 0 & \ddots & \\ 0 & & & T \\ 1 & 1-T & \dots & 1-T \end{bmatrix}$$

which is a product of Burau matrices.

So for any $j \in \mathbf{N} \cup \{0\}$ with $0 \leq j \leq k$, the color vectors after the braid word $(\sigma_{n-1}\sigma_{n-2}\dots\sigma_1)^j$ is $[a_1, a_2, \dots, a_n]A^j = (\sum_{i=1}^n a_i e_i)A^j = \sum_{i=1}^n a_i (e_i A^j)$. Thus any choice of color vectors induces nontrivial color of L if $\sum_{i=1}^n a_i (e_i A^j) = \sum_{i=1}^n a_i e_i$, which occurs if and only if $e_i A^j = e_i$ for every $i = 1, 2, \dots, n$. Note that this is equivalent to $A^j = I$.

5.1 Definition. The *color period* of a quandle Q for the family $\mathcal{T}(n) = \{T(n, m) : m \in \mathbf{Z}\}$ is the minimum positive integer k such that $A^k = I$.

5.2 Lemma. If $e_n A^{kn} = e_n$ for some $k \in \mathbf{Z}$, then $e_j A^{kn} = e_j$ for all $j = 1, 2, \dots, n$.

Proof. Let $e_n A^{kn} = e_n$. Then $e_n A^{(k-1)n+1} = K e_1$ for some $K \in Q$. Since $e_j A = T e_{j+1}$ for $j = 1, 2, \dots, n-1$,

$$e_n A^{kn} = e_n A^{(k-1)n+1} A^{n-1} = K e_1 A^{n-1} = K T^{n-1} e_n = e_n.$$

Hence, $K T^{n-1} = 1$.

Now consider $e_j A^{kn}$ for $j \in \{1, 2, \dots, n\}$. Then,

$$e_j A^{kn} = (e_j A^{n-j}) A^{(k-1)n+j} = T^{n-j} (e_n A^{(k-1)n+1}) A^{j-1} = T^{n-j} K e_1 A^{j-1} = T^{n-j+j-1} K e_j = e_j. \square$$

5.3 Proposition. For A as above, the color periods, p , of the following quandles Q for the family $\mathcal{T}(n) = \{T(n, m) : m \in \mathbf{Z}\}$ are:

- $Q = \mathbf{Z}_8[T, T^{-1}]/(T-3)$, $p = \begin{cases} 2n & \text{if } n = 2k+1, \quad k \in \mathbf{N}, \\ 4n & \text{if } n = 2k, \quad k \in \mathbf{N}. \end{cases}$
- $Q = \mathbf{Z}_3[T, T^{-1}]/(T^2+1)$, $p = \begin{cases} 2n & \text{if } n = 4k+2, \quad k \in \mathbf{N}, \\ 3n & \text{if } n = 4k, \quad k \in \mathbf{N}, \\ 4n & \text{otherwise.} \end{cases}$
- $Q = \mathbf{Z}_3[T, T^{-1}]/(T^2-1)$, $p = \begin{cases} 2n & \text{if } n = 2k+1, \quad k \in \mathbf{N}, \\ 3n & \text{if } n = 2k, \quad k \in \mathbf{N}. \end{cases}$
- $Q = \mathbf{Z}_2[T, T^{-1}]/(T^3-1)$, $p = \begin{cases} 2n & \text{if } n = 3k, \quad k \in \mathbf{Z}, \\ 3n & \text{otherwise.} \end{cases}$
- $Q = \mathbf{Z}_2[T, T^{-1}]/(T^2+T+1) = S_4$, $p = \begin{cases} 2n & \text{if } n = 3k, \quad k \in \mathbf{Z}, \\ 3 & \text{if } n = 2, \\ 3n & \text{otherwise.} \end{cases}$

- $Q = R_j$ for $j = 2k, k \in \mathbf{N}$, $p = \begin{cases} 2n & \text{if } n = 2k + 1, \quad k \in \mathbf{N}, \\ kn & \text{if } n = 2k, \quad k \in \mathbf{N}. \end{cases}$
- $Q = \begin{cases} \mathbf{Z}_8[T, T^{-1}]/(T - 5), \text{ or} \\ \mathbf{Z}_2[T, T^{-1}]/(T^2 + 1) \end{cases}, p = 2n.$
- $Q = \begin{cases} \mathbf{Z}_9[T, T^{-1}]/(T - 4), \text{ or} \\ \mathbf{Z}_9[T, T^{-1}]/(T - 7), \text{ or} \\ \mathbf{Z}_3[T, T^{-1}]/(T^2 + T + 1) \end{cases}, p = 3n.$

Proof. We prove the cases $Q = \mathbf{Z}_2[T, T^{-1}]/(T^2 + T + 1) = S_4$, $Q = \mathbf{Z}_3[T, T^{-1}]/(T^2 + 1)$, and $Q = R_j$ for $j \in \mathbf{N}$. The rest are similar.

First consider $Q = \mathbf{Z}_2[T, T^{-1}]/(T^2 + T + 1) = S_4$, and let $n = 3k$ for some $k \in \mathbf{N}$.

Consider $e_n A = [1, 1 - T, \dots, 1 - T]$. Denote by $q_b(a)$ the operation $a * b$ in S_4 . Note that

$$[a_1, a_2, \dots, a_n]A = [a_n, q_{a_n}(a_1), q_{a_n}(a_2), \dots, q_{a_n}(a_{n-1})]$$

and that $q_b^3(a) = (q_b \circ q_b \circ q_b)(a) = a$ for all $a, b \in S_4$. Hence

$$e_n A^n = [1 - T, \dots, 1 - T, q_{1-T}^{n-1}(1)] = [1 - T, \dots, 1 - T, T].$$

Furthermore,

$$e_n A^{n+1} = [T, q_T(1 - T), \dots, q_T(1 - T)] = [T, 0, \dots, 0],$$

and

$$e_n A^{2n} = [0, \dots, 0, q_0^{n-1}(T)] = [0, \dots, 0, 1] = e_n.$$

Hence, since $e_n A^p \neq e_n$ for any $0 < p < 2n$ and $e_i A^{2n} = e_i$ for all $i = 1, 2, \dots, n$ by the preceding Lemma, the color period is $2n$.

Now consider $n = 3k + 1$ for some $k \in \mathbf{N} \cup \{0\}$. Again, consider $e_n A = [1, 1 - T, \dots, 1 - T]$. Note that

$$e_n A^n = [1 - T, \dots, 1 - T, q_{1-T}^{n-1}(1)] = [1 - T, \dots, 1 - T, 1],$$

and so $e_n A^{n+1} = [1, T, \dots, T]$. Thus, $e_n A^{2n} = [T, \dots, T, 1]$, which leads to $e_n A^{2n+1} = e_1$. From this, it can be seen that

$$e_n A^{3n} = T^{n-1} e_n = T^{3k+1-1} e_n$$

for some $k \in \mathbf{Z}$. Thus $e_n A^{3n} = T^{3k} e_n = e_n$. Thus the color period is $3n$.

For $n = 3k + 2$ for some $k \in \mathbf{N} \cup \{0\}$. Again, consider $e_n A = [1, 1 - T, \dots, 1 - T]$. Note

$$e_n A^n = [1 - T, \dots, 1 - T, q_{1-T}^{n-1}(1)] = [1 - T, \dots, 1 - T, 0],$$

and so $e_n A^{n+1} = [0, 1, \dots, 1]$, which is e_n when $n = 2$. Thus, $e_n A^{2n} = [1, \dots, 1, T + 1]$, which leads to $e_n A^{2n+1} = (T + 1)e_1 = T^2 e_1$. From this, it can be seen that

$$e_n A^{3n} = T^{2+(n-1)} e_n = T^{n+1} e_n = T^{3k+2+1} e_n = e_n$$

since $n = 3k + 2$ for some $k \in \mathbf{Z}$. Thus the color period here is $3n$.

For $Q = \mathbf{Z}_3[T, T^{-1}]/(T^2 + 1)$, we proceed as with S_4 . If $n \equiv 0 \pmod{4}$, then we have the following computations.

$$\begin{aligned}
e_n A &= [1, 1 - T, \dots, 1 - T] \\
&= [1, 1 + 2T, \dots, 1 + 2T] \\
e_n A^n &= [2T + 1, \dots, 2T + 1, 2T + 2] \\
e_n A^{n+1} &= [2T + 2, T + 2, \dots, T + 2] \\
e_n A^{2n} &= [T + 2, \dots, T + 2, T] \\
e_n A^{2n+1} &= [T, 0, \dots, 0].
\end{aligned}$$

Thus, $e_n A^{3n} = e_n$. So for $n \equiv 0 \pmod{4}$, the color period of a n -strand torus link is $3n$. Now let $n \equiv 2 \pmod{4}$. Then $e_n A^n = [2T + 1, 2T + 1, \dots, 2T]$, and so $e_n A^{n+1} = 2Te_1$. Thus $e_n A^{2n} = e_n$. So, the color period is $2n$. For $n \equiv 1 \pmod{4}$, one computes

$$\begin{aligned}
e_n A^n &= [2T + 1, \dots, 2T + 1, 1] \\
e_n A^{n+1} &= [1, 2, \dots, 2] \\
e_n A^{2n} &= [2, \dots, 2, 1] \\
e_n A^{2n+1} &= [1, T + 1, \dots, T + 1] \\
e_n A^{3n} &= [T + 1, \dots, T + 1, 1] \\
e_n A^{3n+1} &= [1, 0, \dots, 0].
\end{aligned}$$

Hence, $e_n A^{4n} = e_n$. For $n \equiv 3 \pmod{4}$, one computes

$$\begin{aligned}
e_n A^n &= [2T + 1, \dots, 2T + 1, T + 1] \\
e_n A^{n+1} &= [T + 1, T, \dots, T] \\
e_n A^{2n} &= [T, \dots, T, T + 2] \\
e_n A^{2n+1} &= [T + 2, 2T + 2, \dots, 2T + 2] \\
e_n A^{3n} &= [2T + 2, \dots, 2T + 2, 2] \\
e_n A^{3n+1} &= [2, 0, \dots, 0]
\end{aligned}$$

Hence, $e_n A^{4n} = e_n$. Thus the color periods are $4n$.

Finally, for $Q = R_j$ for $j = 2k, k \in \mathbf{N}$, note that Q is isomorphic to $\mathbf{Z}_j[T, T^{-1}]/(T + 1)$. So, $T = -1$, which makes $1 - T = 2$, so $e_n A = [1, 2, \dots, 2]$. If n is odd, $e_n A^n = [2, \dots, 2, 1]$, so $e_n A^{n+1} = [1, 0, \dots, 0]$. This means that $e_n A^{2n} = e_n$. Thus the color period is $2n$. If n is even $e_n A^n = [2, \dots, 2, 3]$. Noting that $n * (n + 1) = n + 2$, for $i = 1, 2, \dots, k$ we will get

$$\begin{aligned}
e_n A^{in} &= [2i, \dots, 2i, 2i + 1], \\
e_n A^{in+1} &= [2i + 1, 2i + 2, \dots, 2i + 2].
\end{aligned}$$

When $i = k - 1, 2i + 2 = 2(k - 1) + 2 = 2k = j \equiv 0 \pmod{j}$, and so $e_n A^{nk} = e_n$. \square

5.4 Proposition. *Let p be the color period of a quandle Q for the family $\mathcal{T}(n)$. Let $\theta \in Z^2(Q, \mathbf{Z}_q)$. Then $\Phi_\theta(T(n, k))$ is periodic with respect to k with period at most pq .*

Proof. Let Q be a quandle that has color period p with respect to $\mathcal{T}(n)$. Then any torus knot or link $T(n, s)$ with $s > p$, $s = ph + r$ ($0 \leq r < p$), can be thought of as the closure of a finite number (h) of the block $(\sigma_{n-1}\sigma_{n-2}\dots\sigma_1)^p$ and a remainder block $(\sigma_{n-1}\sigma_{n-2}\dots\sigma_1)^r$. It has been shown that the color vector after the p th block is the same as the initial (at the top of the braid representation) color vector. Hence the $(ph + r)$ -th color vector is the same as the r -th color vector for $r = 1, 2, \dots, p - 1$. Let v be an initial color vector which colors $T(n, s)$. Let t^α and t^β be the contribution of to the state-sum of $(\sigma_{n-1}\sigma_{n-2}\dots\sigma_1)^p$ and $(\sigma_{n-1}\sigma_{n-2}\dots\sigma_1)^r$ respectively, for the color with the initial color vector v . Then the contribution of $(\sigma_{n-1}\sigma_{n-2}\dots\sigma_1)^s$ is $t^{\alpha h + \beta}$ since $s = ph + r$. Hence if $h = q$ (with $A = \mathbf{Z}_q$), we obtain $t^{\alpha h + \beta} = t^\beta$, and therefore $\Phi(T(n, ph + r)) = \Phi(T(n, r))$. \square

5.5 Example. The above Proposition implies that the invariants $\Phi(T(n, r))$ for $0 \leq r < pq$ determine all the rest of $\Phi(T(n, s))$. Here we present the list of $\Phi(T(2, s))$, for a cocycle in $Z^2(\mathbf{Z}_8[T, T^{-1}]/(T - 5), \mathbf{Z}_2)$ (as this quandle displays a variety of polynomial values). In this case the period pq is 8. In the following table, k represents any integer. The cocycle used is

$$\phi = \chi_{0,1} + \chi_{0,5} + \chi_{1,5} + \chi_{2,1} + \chi_{2,5} + \chi_{3,5} + \chi_{5,1} + \chi_{7,1}.$$

torus link	invariant
$T(2, 8k)$	64
$T(2, 1 + 8k)$	8
$T(2, 2 + 8k)$	$28 + 4t$
$T(2, 3 + 8k)$	8
$T(2, 4 + 8k)$	$48 + 16t$
$T(2, 5 + 8k)$	8
$T(2, 6 + 8k)$	$28 + 4t$
$T(2, 7 + 8k)$	8

5.6 Table. The following table presents calculations of $\Phi(T(n, k))$ with some quandles for some small values of k . The quandles are Alexander quandles with $A = \mathbf{Z}_q$. Although they do not give complete set of initial conditions (as the periods pq are sometimes too large), they give useful information together with the proposition above. The table lists $\Phi(T(n, k))$ for $n \leq k$ since $T(n, k) = T(k, n)$.

We used the following cocycles:

$$\begin{aligned} \Theta_1 &= \chi_{0,2} + \chi_{1,0} + \chi_{1,2} + \chi_{2,0} \\ \Theta_2 &= \chi_{0,3} + \chi_{4,1} + \chi_{2,5} + \chi_{2,3} + \chi_{2,1} + \chi_{1,5} + \chi_{1,3} + \chi_{3,5} + \chi_{3,1} \\ \Theta_3 &= \chi_{0,4} + \chi_{2,4} + \chi_{2,0} + \chi_{4,0} + \chi_{3,4} + \chi_{3,2} + \chi_{4,2} + \chi_{5,0} \\ &\quad + \chi_{2,6} + \chi_{3,0} + \chi_{3,6} + \chi_{4,6} + \chi_{5,2} + \chi_{6,2} + \chi_{1,6} + \chi_{1,4} \\ \Theta_4 &= \chi_{1,0} + \chi_{T,0} \\ \Theta_5 &= \chi_{0,1} + \chi_{0,T} + \chi_{1,0} + \chi_{1,T} + \chi_{T,0} + \chi_{T,1} \\ \Theta_6 &= \chi_{1,0} + 2\chi_{0,2} + \chi_{0,1} + 2\chi_{2,1} + \chi_{1,2} + 2\chi_{0,T} + \chi_{1,T+1} + \chi_{T,0} + 2\chi_{T,1} + \chi_{T+1,T} \end{aligned}$$

$$\begin{aligned}
& + \chi_{2+T,T+1} + 2\chi_{2+T,T} + 2\chi_{2T,0} + 2\chi_{2+T,1+2T} + \chi_{2+T,2T} + \chi_{2T,T+1} \\
& + \chi_{2T,2} + 2\chi_{2T,1} + \chi_{1+2T,0} + 2\chi_{0,2+2T} + \chi_{2T,1+2T} + \chi_{0,2T} + 2\chi_{0,2+T} \\
& + 2\chi_{0,T+1} + 2\chi_{2T,2+T} + \chi_{1,2T} + 2\chi_{1+2T,T+1} + \chi_{1+2T,T} + \chi_{1+2T,2} \\
& + \chi_{1+2T,1} + 2\chi_{1,2+2T} + \chi_{2,2T} + \chi_{2,2+T} + 2\chi_{2+2T,2} + \chi_{2,T+1} + \chi_{2,T} \\
& + \chi_{2+2T,2+T} + 2\chi_{T,2} + 2\chi_{T,2+T} + 2\chi_{T,T+1} + 2\chi_{T,1+2T} + \chi_{T,2T} + \chi_{T+1,1} \\
& + \chi_{T+1,2} + 2\chi_{T+1,2+T} + 2\chi_{T+1,2T} + 2\chi_{T+1,1+2T} + 2\chi_{2+T,0} + \chi_{2+T,1} \\
\Theta_7 = & \chi_{0,1} + \chi_{2,1} + \chi_{0,T} + \chi_{1,T} + \chi_{2+T,T} + \chi_{2+T,2+2T} + \chi_{2T,1} + \chi_{1,2+2T} + \chi_{2+2T,T} + \chi_{2,T} \\
& + \chi_{2+2T,1} + \chi_{2,2+2T} + \chi_{T+1,2+2T} \\
\Theta_8 = & \chi_{0,1} + \chi_{0,T} + \chi_{0,2+2T} + 2\chi_{1,T} + \chi_{1,2+2T} + 2\chi_{2,1} + \chi_{2,2+2T} + \chi_{T,1} + 2\chi_{T,2+2T} \\
& + \chi_{T+1,T} + 2\chi_{T+1,2+2T} + 2\chi_{2+T,1} + 2\chi_{2+T,T} + 2\chi_{2+T,2+2T} + \chi_{2T,1} \\
& + 2\chi_{2T,T} + 2\chi_{2+2T,1} + \chi_{2+2T,T} \\
\Theta_9 = & \chi_{0,1} + \chi_{0,5} + \chi_{1,5} + \chi_{2,1} + \chi_{2,5} + \chi_{3,5} + \chi_{5,1} + \chi_{7,1} \\
\Theta_{10} = & \chi_{0,1} + \chi_{0,4} + \chi_{0,7} + \chi_{3,1} + \chi_{3,4} + \chi_{3,7} + \chi_{6,1} + \chi_{6,4} + \chi_{6,7}
\end{aligned}$$

quandle Q	cocycle	A	T(n,k)	invariant
R_4	Θ_1	\mathbf{Z}_2	$T(2, 4)$	$8 + 8t$
			$T(4, 6)$	$8 + 8t$
			$T(4, 8)$	$128 + 128t$
R_6	Θ_2	\mathbf{Z}_2	$T(2, 2)$	$6 + 6t$
			$T(2, 6)$	$18 + 18t$
			$T(4, 4)$	$216 + 216t$
			$T(4, 12)$	$648 + 648t$
R_8	Θ_3	\mathbf{Z}_2	$T(2, 8)$	$32 + 32t$
			$T(4, 16)$	$2048 + 2048t$
$\mathbf{Z}_2[T, T^{-1}]/(T^2 + 1)$	Θ_4	\mathbf{Z}_2	$T(2, 4)$	$8 + 8t$
			$T(4, 6)$	$8 + 8t$
			$T(4, 8)$	$128 + 128t$
$\mathbf{Z}_2[T, T^{-1}]/(T^2 + T + 1)$	Θ_5	\mathbf{Z}_2	$T(2, 3)$	$4 + 12t$
			$T(3, 3)$	$4 + 12t$
			$T(3, 6)$	$16 + 48t$
$\mathbf{Z}_3[T, T^{-1}]/(T^2 + 1)$	Θ_6	\mathbf{Z}_3	$T(2, 4)$	$9 + 36t + 36t^2$
			$T(4, 4)$	$297 + 216t + 216t^2$
			$T(4, 8)$	$297 + 216t + 216t^2$
			$T(4, 10)$	$9 + 36t + 36t^2$
$\mathbf{Z}_3[T, T^{-1}]/(T^2 - 1)$	Θ_7	\mathbf{Z}_2	$T(2, 2)$	$21 + 6t$
			$T(2, 6)$	$63 + 18t$
			$T(3, 3)$	$63 + 18t$
			$T(4, 4)$	$1647 + 540t$
			$T(4, 12)$	$4941 + 1620t$
$\mathbf{Z}_3[T, T^{-1}]/(T^2 + T + 1)$	Θ_8	\mathbf{Z}_3	$T(3, 3)$	$135 + 54t + 54t^2$
			$T(3, 6)$	$135 + 54t + 54t^2$
$\mathbf{Z}_8[T, T^{-1}]/(T - 5)$	Θ_9	\mathbf{Z}_2	$T(2, 2)$	$28 + 4t$
			$T(2, 4)$	$48 + 16t$
			$T(2, 6)$	$28 + 4t$
			$T(3, 3)$	$104 + 24t$
			$T(4, 4)$	$1600 + 448t$
			$T(4, 6)$	$48 + 16t$
			$T(4, 6)$	$3072 + 1024t$
$\mathbf{Z}_9[T, T^{-1}]/(T - 7)$	Θ_{10}	\mathbf{Z}_2	$T(2, 6)$	$63 + 18t$
			$T(3, 3)$	$81 + 162t$
			$T(3, 9)$	$567 + 162t$
			$T(4, 12)$	$4941 + 1620t$

Table 5.6 : Nontrivial invariants of torus links

6 Computations with Movies

In this section we present a method of computing the cocycle invariants using movies, with a sample calculation for a deform-spun figure-8 knot, the movie of which is illustrated in Fig. 8.

First, we describe the knotted sphere that the movie illustrates. The sequence of *stills* consist of classical knot diagrams. Successive stills differ by a Reidemeister move of type II or III, a critical point of the surface, or a planar isotopy of the underlying diagram. Type I moves are not used in this particular example, though they may appear in general. Exceptions are made for maximal/minimal points (or the birth/death of small circles) where dots are depicted in some stills in the figure to make clear where they occurred. In this case, the exact moment of critical points are depicted in a still, instead of between successive stills. The entries in the figure are referred to by a pair of numbers that indicate the row and column in the figure. Thus still (1,8) is a standard picture of the connected sum of a pair of figure-8 knots.

Stills (1,1), (1,2), (6,7), and (6,8) represent critical levels in which simple closed curves are born or die. In particular, the still (1,1) consists of a single dot where a birth occurs. The still (1,2) consists of one circle and a dot.

These curves are colored a and b with the curve colored b nested inside the curve colored a . Other critical points (saddle points) occur between stills (1,7) and (1,8) and between (6,1) and (6,2). Since these are all the critical points the resulting surface depicted is a sphere.

The labels indicate a coloring of the diagram by S_4 . It is seen that for any $a, b \in S_4$, if $d = a * b$ and $c = b * d$, then such a choice gives a coloring. In particular, there is a non-trivial coloring of this knotted surface by S_4 . The quandle rule holds at each crossing point of the stills. As the crossings move from still to still, they sweep out double point arcs, and the quandle coloring rule holds along these double point arcs. The non-trivial colorings show that the quandle of the embedded sphere is non-trivial, and so the sphere is indeed knotted. Observe that the proof of knotting does not depend on an *a priori* knowledge that the sphere is deform-spun knot.

Next we describe the story-board of the movie. Roughly the second, third, fourth rows each involve pushing the top figure-8 tangle past an arc of the bottom figure-8 tangle. The figure is arranged to fit on a page, and so at the end of the first and second rows the top knot has begun its next migration. Each of the four crossings of the top figure-8 tangle must cross under or over one of the four arcs of the bottom figure-8 tangle. When the crossings past these arcs triple points in the projection occur. The triple points appear as Reidemeister type III moves between the stills. There are 16 such triple points they occur in the scenes listed in the table below.

Most of the rest of the changes are type II Reidemeister moves. The exceptions are (2,6) \mapsto (2,7), where a rescaling has taken place, and (4,7) \mapsto (5,1), where the bottom tangle has rotated clockwise around the left most arc to become the top tangle in (5,1).

One can use the movie to obtain the following presentation of the quandle of the knotted sphere.

$$\langle x, y : y * (x * \bar{y}) = x * y; y * (y * (x * \bar{y})) = x \rangle.$$

In order to evaluate the cocycle invariant for cocycles in $Z^3(S_4, A)$, we need to examine the signs of the triple points and the colors of the regions away from which the normal point. This examination is easily made by comparing the given scenes in the movie with the Reidemeister type III moves that are illustrated in Fig. 9. This figure illustrates the 96 possible type III moves (48 in

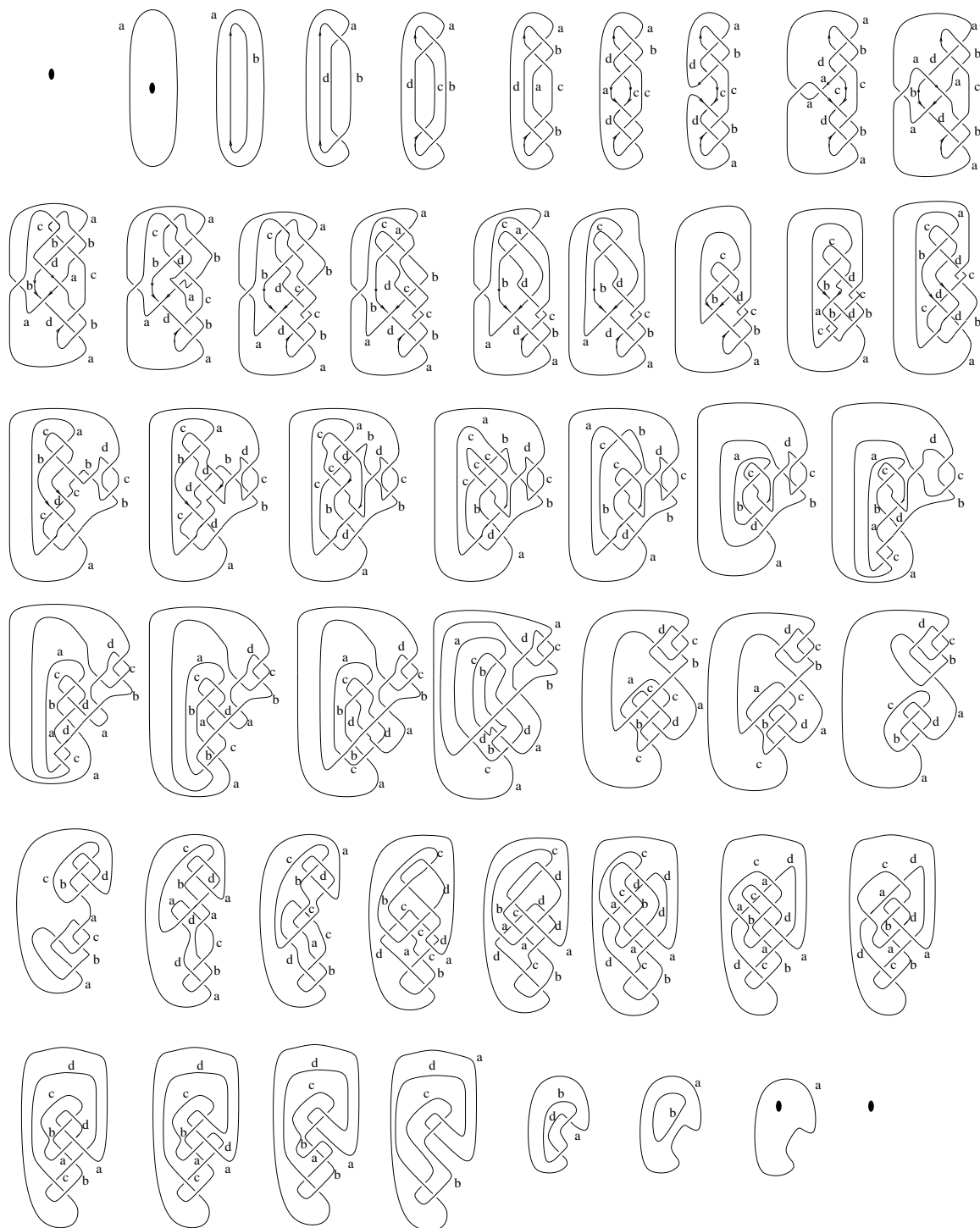


Figure 8: A deform spun figure eight knot

Figure 9: All possibilities of oriented type III moves

the direction of the arrows, 48 in the opposite direction). The black dots indicate the region into which all normals point when the normal points to the left of the oriented arc. The labels (p, q, r) indicate the colors on the bottom, middle, and top (resp.) sheets that are the arguments of the quandle cocycles. The entries in Fig. 9 are indicated in a manner similar to those in the previous figure. Thus in entry (1,6) the braid move $\sigma_1\sigma_2\sigma_1 \mapsto \sigma_2\sigma_1\sigma_2$ is indicated.

In the following table we indicate the scenes that correspond to triple points, the entry in Fig. 9 to which the scenes correspond. The third column indicates whether the entry in the figure is read forward (left to right) or backward (right to left). If it is backward then the sign of the triple point is opposite to that indicated in the figure. The last column indicates the Boltzmann weight associated to the triple point in the movie Fig. 8.

Scene in movie	type III	direction	Weight
(1, 9) \mapsto (1, 10)	(1, 2)	\leftarrow	$\theta(b, a, a)^{-1}$
(2, 1) \mapsto (2, 2)	(2, 5)	\rightarrow	$\theta(c, b, a)$
(2, 2) \mapsto (2, 3)	(2, 4)	\rightarrow	$\theta(c, d, a)^{-1}$
(2, 3) \mapsto (2, 4)	(1, 4)	\rightarrow	$\theta(b, c, a)$
(2, 8) \mapsto (2, 9)	(5, 4)	\rightarrow	$\theta(c, b, a)^{-1}$
(3, 1) \mapsto (3, 2)	(6, 1)	\rightarrow	$\theta(d, c, d)^{-1}$
(3, 2) \mapsto (3, 3)	(6, 4)	\rightarrow	$\theta(c, c, b)$
(3, 3) \mapsto (3, 4)	(5, 1)	\rightarrow	$\theta(c, b, c)$
(4, 1) \mapsto (4, 2)	(1, 6)	\rightarrow	$\theta(b, a, b)$
(4, 2) \mapsto (4, 3)	(2, 3)	\rightarrow	$\theta(c, d, b)$
(4, 3) \mapsto (4, 4)	(2, 6)	\rightarrow	$\theta(c, b, b)^{-1}$
(4, 4) \mapsto (4, 5)	(1, 3)	\rightarrow	$\theta(b, c, b)^{-1}$
(5, 2) \mapsto (5, 3)	(2, 6)	\leftarrow	$\theta(a, b, c)$
(5, 4) \mapsto (5, 5)	(4, 5)	\leftarrow	$\theta(d, d, a)$
(5, 5) \mapsto (5, 6)	(2, 4)	\rightarrow	$\theta(c, d, b)^{-1}$
(5, 6) \mapsto (5, 7)	(1, 1)	\rightarrow	$\theta(c, b, d)^{-1}$

Recall from [4] that the following are non-trivial 3-cocycles for S_4 with various coefficients.

$$\begin{aligned}
\eta_1 &= +\chi_{(0,1,0)} + \chi_{(0,2,1)} + \chi_{(0,2,3)} + \chi_{(0,3,0)} + \chi_{(0,3,1)} + \chi_{(0,3,2)} + \chi_{(1,0,1)} \\
&\quad + \chi_{(1,0,3)} + \chi_{(1,2,0)} + \chi_{(1,3,1)} + \chi_{(2,0,3)} + \chi_{(2,1,0)} + \chi_{(2,1,3)} + \chi_{(2,3,2)}; \\
\eta_2 &= +\chi_{(0,1,2)} - \chi_{(0,1,3)} - \chi_{(0,2,1)} + \chi_{(0,3,0)} + \chi_{(0,3,1)} - \chi_{(0,3,2)} + 2\chi_{(1,0,1)} \\
&\quad + \chi_{(1,0,2)} + \chi_{(1,0,3)} - \chi_{(1,2,0)} + \chi_{(1,3,2)} + \chi_{(2,0,1)} + \chi_{(2,0,2)} + \chi_{(2,0,3)} \\
&\quad + \chi_{(2,1,3)} + \chi_{(3,0,1)} + \chi_{(3,0,2)} + \chi_{(3,0,3)} + \chi_{(3,1,3)}; \\
\eta_{11} &= -\chi_{(0,1,0)} - \chi_{(0,1,3)} + \chi_{(0,3,1)} + \chi_{(0,3,2)} - \chi_{(1,0,1)} - \chi_{(1,0,2)} - \chi_{(1,0,3)} \\
&\quad + \chi_{(1,2,0)} - \chi_{(1,2,1)} + \chi_{(1,3,0)} + \chi_{(1,3,1)} + \chi_{(1,3,2)} + \chi_{(2,0,3)} - \chi_{(2,1,0)} - \chi_{(3,0,2)} + \chi_{(3,2,3)}
\end{aligned}$$

Thus we have

6.1 Theorem. *The state sum invariants for the deform-spun figure-8 knot that is depicted in Fig. 8 is*

$$\Phi_\theta = \sum \theta(b, c, a)\theta(c, b, c)\theta(b, a, b)\theta(a, b, c)\theta(c, d, a)^{-1}\theta(d, c, d)^{-1}\theta(b, c, b)^{-1}\theta(c, b, d)^{-1}$$

where the sum is taken over all pairs of elements $a, b \in S_4$ and $a = d * b$ while $c = b * d$. We have the values

- $\Phi_{\eta_{11}} = 16$.
- $\Phi_{\eta_1} = 4 + 12t$ for t a generator of \mathbf{Z}_2 .
- $\Phi_{2\eta_1} = 4 + 12t^2$ for t a generator of \mathbf{Z}_4 .
- $\Phi_{\eta_2} = 4 + 12t$ for t a generator of \mathbf{Z}_2 .
- $\Phi_{\eta_2} = 4 + 12t$ for t a generator of \mathbf{Z}_4 .

7 Twist-spun Torus Knots

Let $\tau^k T(p, q)$ denote the k -twist spun (p, q) -torus knot (or link). The construction of twist spun knots was first defined by Zeeman [42], see also [40]. In this section we use movies to compute the state-sum expressions of $\tau^k T(2, m)$ with cocycles over dihedral quandles. We prove the invariants are periodic with respect to k . Then we evaluate the state-sum for some quandle cocycles with various coefficients. First we establish some notation.

7.1 Notation. Let x, y denote elements of an Alexander quandle $\Lambda = \mathbf{Z}_p[T, T^{-1}]/(f(T))$; let s denote an integer. Define quandle elements $G(s) = G(x, y, s, T)$ recursively by

$$\begin{aligned} G(-1) &= x \\ G(0) &= y \\ G(s+1) &= TG(s-1) + (1-T)G(s) \end{aligned}$$

Then $G(-2) = T^{-1}y + (1 - T^{-1})x$, and for $s \geq 0$,

$$G(s) = x \sum_{j=1}^s (-1)^{j+1} T^j + y \sum_{j=0}^s (-1)^j T^j.$$

Define $h(x, y, 0) = y$, and $h(x, y, n) = T^{-n}y + (1 - T^{-n})x$. Then h satisfies the relation $Th(x, y, n+1) + (1 - T)x = h(x, y, n)$.

If θ is a 3-cocycle for the quandle Λ , then define

$$\Theta_0^m(x, y, T) = \prod_{j=0}^{m-1} \theta(G(x, y, -2, T), G(x, y, j-1, T), G(x, y, j, T))^{-1}.$$

and

$$\Theta_1^m(x, y, T) = \prod_{j=0}^{m-1} \theta(G(x, y, j-2, T), G(x, y, j-1, T), G(x, y, -2, T)).$$

Next we describe the important scenes in the movie of the twist-spun torus knots, $\tau^k T(2, m)$. The tangle depicted in Fig. 10 is the tangle of $T(2, m)$ upon which we will apply the twisting. The initial stages of the first half-twist are indicated in Figs. 10 and 11. The final stages of the half-twist are indicated in Fig. 12. In Fig. 10 quandle elements are indicated on the center arcs of the torus tangle. After the s th crossing the arc on the right of the crossing is colored $G(s)$. The normal direction to the surface is chosen to be a right pointing arrow on arcs that run downward. On the right-hand side of Fig. 11 a new arc with color $G(-2)$ is born via a type II Reidemeister move. The asterisk in the triangle indicates the location of a type III Reidemeister move that is about to take place. Compare this to Fig. 9 entry (2,6). This and the subsequent type III Reidemeister moves during the first half-twist are all of this type; the signs are all negative. The arguments for the cocycles are indicated in Fig. 11 where the relationship between the arguments on subsequent type III moves is indicated by the crossed arrows. The second half-twist is indicated in Figs. 13 through 16. Here the type III move appears in Fig. 9 as entry (6,6).

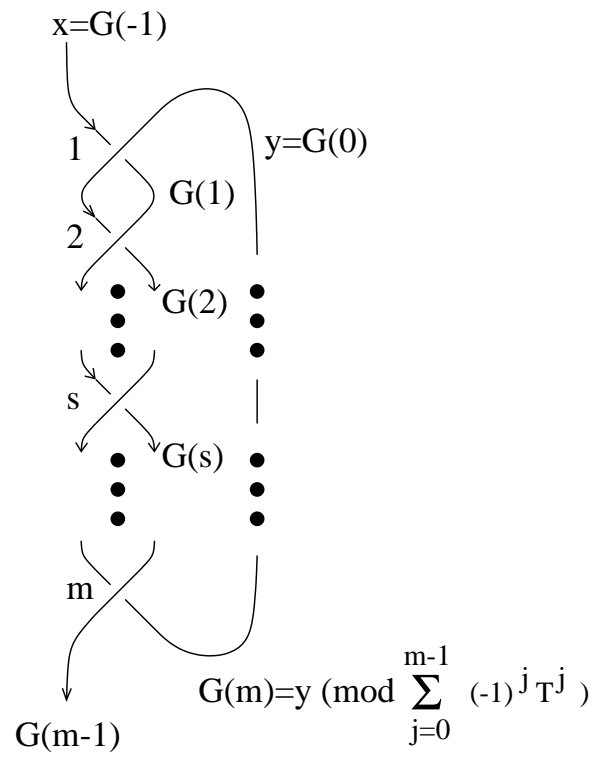


Figure 10: Alexander colors for $\tau^k T(2, m)$

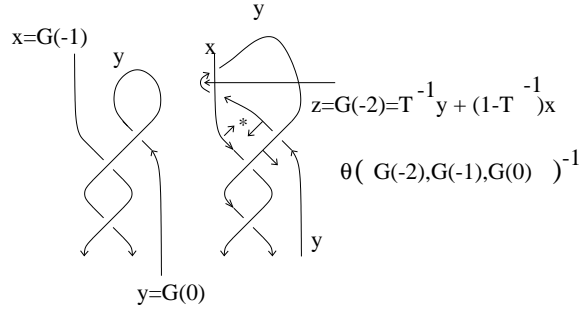


Figure 11: Start twisting on top

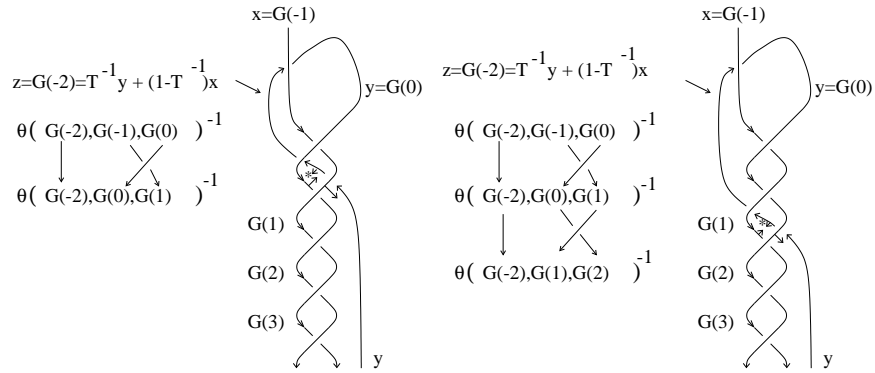


Figure 12: Continue twisting by Reidemeister III moves

7.2 Theorem. *The surface $\tau^k T(2, m)$, with the orientation shown in Fig. 10, colors nontrivially with the Alexander rack $\Lambda = \mathbf{Z}_p[T, T^{-1}]/(f(T))$ if and only if $1 - T + \dots \pm T^{m-1} = 0$ and $T^k = 1$ in Λ .*

The state-sum invariant of $\tau^k T(2, m)$ with a cocycle θ of the Alexander quandle Λ is

$$\sum_{x, y} \prod_{n=0}^{k-1} \Theta_0^m(x, h(x, y, n), T) \Theta_1^m(x, h(x, y, n), T)$$

Proof. As discussed above, Fig. 10 through Fig. 16 depict one full twist of a diagram of $T(2, m)$ by a sequence of Reidemeister moves. First, Fig. 10 shows that $T(2, m)$ is non-trivially colored by Λ if and only if $G(s) = G(x, y, m, T) = x \sum_{j=1}^m (-1)^{j+1} T^j + y \sum_{j=0}^m (-1)^j T^j = y$ if and only if $\sum_{j=1}^m (-1)^{j+1} T^j = 0$ in Λ . After one full twist, the color on the right-hand arc of the figures changes to $h(x, y, 1) = T^{-1}y + (1 - T^{-1})x$. By induction, the color on the right-hand arc after k full twists is $h(x, y, k) = T^{-k}y + (1 - T^{-k})x$. Hence $\tau^k T(2, m)$ is non-trivially colored if and only if $T^k = 1$ in Λ . Note also that the colors on $\tau^k T(2, m)$ are periodic with period k if $T^k = 1$.

After one full twist the Reidemeister type III moves have contributed factors of $\Theta_0^m(x, y, T) \Theta_1^m(x, y, T)$ to a term in the state-sum, and the color $y = h(x, y, 0)$ on the right-hand arc has changed to $h(x, y, 1)$ when the twist is complete. The result follows. \square .

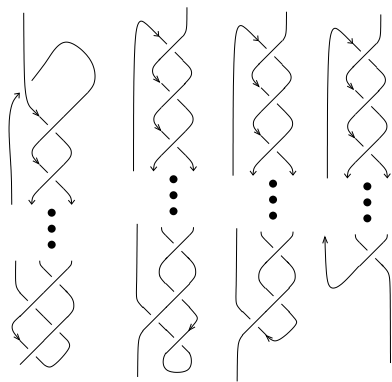


Figure 13: Complete half a twist

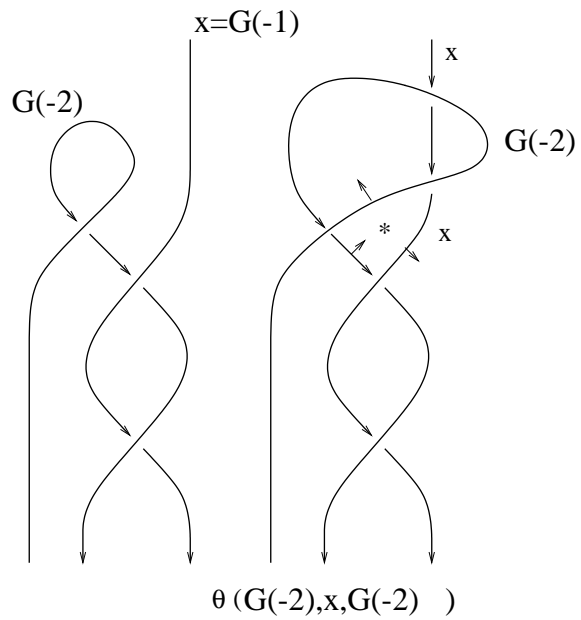


Figure 14: Start twisting again on top

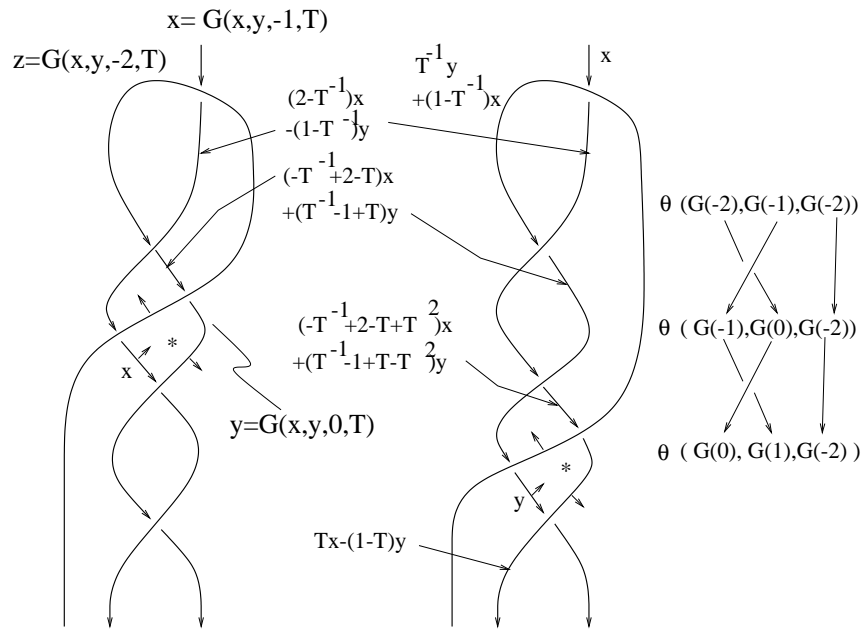


Figure 15: Keep twisting by Reidemeister III moves

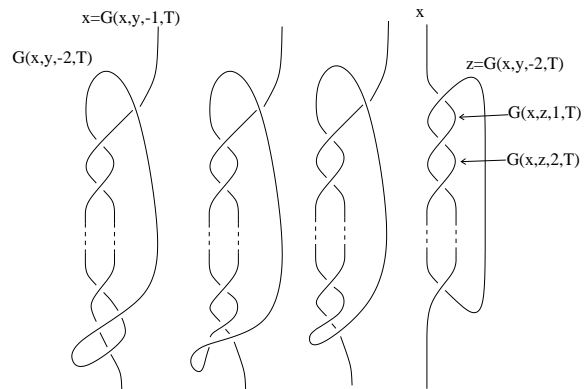


Figure 16: One full twist completed

7.3 Corollary. *Suppose $1 - T + \dots \pm T^{m-1} = 0$ and $T^n = 1$ in the given Alexander rack Λ . Let θ be a 3-cocycle in $Z^3(\Lambda, \mathbf{Z}_q)$. Then $\Phi_\theta(\tau^k T(2, m))$ is periodic with respect to k with period nq .*

Proof. The colors have period n and the state-sum takes values in \mathbf{Z}_q , so the state-sum has period nq . \square

7.4 Corollary. *The surface $\tau^k T(2, m)$ colors nontrivially with the dihedral rack R_h if and only if $h = m$ and $2|k$. The state-sum invariant of $\tau^{2w} T(2, m)$ with a cocycle θ of a dihedral rack R_m is*

$$\begin{aligned} \Phi_\theta(\tau^{2w} T(2, m)) &= \sum_{x,y} \prod_{n=0}^{k-1} \Theta_0^m(x, h(x, y, n), -1) \Theta_1^m(x, h(x, y, n), -1) \\ &= \sum_{x,y} [\Theta_0^m(x, y, -1) \Theta_1^m(x, y, -1)] [\Theta_0^m(x, 2x - y, -1) \Theta_1^m(x, 2x - y, -1)] \\ &\times [\Theta_0^m(x, y, -1) \Theta_1^m(x, y, -1)] [\Theta_0^m(x, 2x - y, -1) \Theta_1^m(x, 2x - y, -1)] \\ &\times \dots \text{a total of } w \text{ factors} \dots \\ &\times [\Theta_0^m(x, y, -1) \Theta_1^m(x, y, -1)] [\Theta_0^m(x, 2x - y, -1) \Theta_1^m(x, 2x - y, -1)] \end{aligned}$$

Furthermore, if the coefficient of the cohomology is $A = \mathbf{Z}_q$, i.e. if $\theta \in C_Q^2(R_m, \mathbf{Z}_q)$, then $\Phi_\theta(\tau^k T(2, m))$ is periodic with respect to k with period $2q$.

Proof. Evaluate $h(x, y, n)$ at $T = -1$ to obtain

$$\begin{aligned} (-1)^{2j} y + (1 - (-1)^{2j}) x &= y, \\ (-1)^{2j+1} y + (1 - (-1)^{2j+1}) x &= 2x - y. \end{aligned}$$

The terms of the state-sum have the form Θ^w so that it has period q . Since the color has period 2, the invariant has period $2q$. \square

7.5 Table. For the rest of the section we present MAPLE computations of the state-sum invariants for twist spun $T(2, m)$ torus knots using the above formulas. Computations are summarized in the following table. The Alexander ideal of $\tau^k T(2, m)$ is $(\Delta_m = T^{m-1} - \dots \pm 1, T^k - 1)$. Somewhat simplified ideals are shown in the table. Since Δ_m divides $T^{2m} - 1$ if m is odd and $T^m - 1$ if m is even, the Alexander modules are periodic with respect to k . Thus we listed up to the smallest period in the table.

The quandles we used are those whose 3-cocycles were computed in Section 3 with non-trivial cohomological dimension. Often there is a pattern that the dimensions are the same for several prime numbers of q . In that case, the smallest among such is chosen.

Since the dihedral quandles R_m and other quandles of the same order appear often as quandles that color $\tau^k T(2, m)$ non-trivially, we listed knots with $m < 7$, as MAPLE does not finish computations for larger quandles in predictable time.

The blank entries means that either only trivial quandles color, or no quandles color. In these cases the invariant column is also left blank.

For $\tau^4 T(2, m)$, the invariant follows from periodicity, since $\tau^2 T(2, m)$ colors with the same quandle R_m . In this case, the same cocycle was used for both knotted surfaces. When the same quandles are used for various k , we applied the periodicity in this way. Such cases are marked by

(p) in the table. The first few examples of such values are provided in the table, but the others are left for the reader.

When there are more than one choice of cocycles that give different values of the invariant, some different choices are made by experiments. In particular, we do not know those listed exhaust all possibilities. The cocycles of choice are presented with the table.

If, for example, $3 + 6t$ is a value of the invariant with $A = \mathbf{Z}_3$, then $3 + 6t^2$ appears also as a value, by taking the negative of the cocycles of the former value. Such cases are listed but cocycles are not given in duplicate.

The choices of cocycles are as follows. The indices in front of cocycles represent indices in the table: $(m - k - A - b)$ represents the invariant for $\tau^k T(2, m)$, the first (represented by $(-A-)$) choice of quandle/coefficient, the second (represented by $(-b)$) choice of a cocycle.

$$\begin{aligned}
(3 - 2 - A) & 2\chi_{0,1,2} + 2\chi_{0,2,1} + 2\chi_{1,0,1} + 2\chi_{1,0,2} + 2\chi_{2,0,1} + 2\chi_{2,0,2} \\
(3 - 3 - A - a) & \chi_{0,T,1+T} + \chi_{0,1+T,1} + \chi_{1,0,1} + \chi_{1,0,T} + \chi_{1,0,1+T} + \chi_{1,T,0} + \chi_{1,T,1} + \chi_{1,1+T,0} \\
& + \chi_{T,0,1} + \chi_{T,0,T} + \chi_{T,1,0} + \chi_{T,1+T,0} \\
(3 - 3 - A - b) & \chi_{1,T,1+T} + \chi_{1,T,0} + \chi_{1,T,1} + \chi_{1,0,1} + \chi_{0,1+T,0} + \chi_{0,T,0} + \chi_{0,T,1} + \chi_{0,1,T} \\
& + \chi_{T,1+T,0} + \chi_{T,0,T} + \chi_{T,0,1+T} + \chi_{1+T,T,1+T} + \chi_{1+T,0,T} + \chi_{1+T,0,1+T} + \chi_{1+T,0,1} \\
(4 - 2 - A - a) & \chi_{0,1,0} + \chi_{0,1,3} + \chi_{0,2,1} + \chi_{0,2,3} + \chi_{0,3,0} + \chi_{0,3,1} \\
(4 - 2 - A - b) & \chi_{0,3,1} + \chi_{0,2,3} + \chi_{0,3,2} + \chi_{0,2,0} + \chi_{2,0,1} + \chi_{2,1,3} + \chi_{2,1,0} + \chi_{2,0,2} \\
(4 - 2 - B - a) & \chi_{0,1,0} + \chi_{0,1,T} + \chi_{0,T,0} + \chi_{0,T,1} + \chi_{0,1+T,1} + \chi_{0,1+T,T} \\
(4 - 2 - B - b) & \chi_{0,1,0} + \chi_{0,1,T} + \chi_{0,T,0} + \chi_{0,T,1} + \chi_{0,1+T,1} + \chi_{0,1+T,T} + \chi_{1,0,1} + \chi_{1,0,1+T} \\
& + \chi_{1,T,0} + \chi_{1,T,1+T} + \chi_{1,1+T,0} + \chi_{1,1+T,1} \\
(5 - 2 - A) & 3\chi_{3,0,2} + 4\chi_{3,0,1} + 3\chi_{3,0,3} + \chi_{3,0,4} + \chi_{3,4,0} + 4\chi_{3,4,3} + 2\chi_{3,1,2} + \chi_{3,1,3} \\
& + 2\chi_{4,0,1} + 3\chi_{4,0,2} + 2\chi_{3,2,1} + 3\chi_{4,0,3} + \chi_{4,0,4} + 2\chi_{0,1,0} + 4\chi_{0,1,2} + 2\chi_{0,1,3} \\
& + 2\chi_{0,1,4} + 2\chi_{0,2,0} + 3\chi_{1,0,1} + \chi_{0,3,1} + \chi_{0,3,2} + 3\chi_{0,4,0} + \chi_{0,4,1} + 4\chi_{1,0,2} \\
& + 3\chi_{1,0,3} + 4\chi_{3,2,4} + 4\chi_{0,4,3} + 3\chi_{0,4,2} + 2\chi_{1,0,4} + 2\chi_{1,3,2} + 2\chi_{1,3,1} + 2\chi_{1,2,4} \\
& + 3\chi_{1,3,0} + 3\chi_{1,2,1} + 2\chi_{1,2,3} + 3\chi_{1,2,0} + 4\chi_{1,3,4} + 3\chi_{1,4,0} + 4\chi_{1,4,1} + \chi_{2,0,2} \\
& + \chi_{2,0,3} + 3\chi_{2,1,2} + 2\chi_{2,1,3} + 4\chi_{2,1,0} + 2\chi_{2,3,0} + 2\chi_{2,1,4} + 2\chi_{2,3,4} + 2\chi_{2,4,0} \\
& + 3\chi_{2,4,1} + 3\chi_{2,3,2} + 4\chi_{2,3,1} + \chi_{2,4,2} + \chi_{4,2,1} \\
(6 - 2 - A) & \chi_{0,1,2} + \chi_{0,2,1} + \chi_{1,0,1} + \chi_{1,0,2} + \chi_{2,0,1} + \chi_{2,0,2} \\
(6 - 2 - B - a) & \chi_{2,3,1} + \chi_{2,3,4} + 2\chi_{2,5,0} + 2\chi_{2,5,3} + \chi_{4,0,2} + \chi_{4,0,5} + \chi_{4,1,2} + \chi_{4,1,5} \\
& + \chi_{4,1,3} + \chi_{4,2,0} + \chi_{4,2,3} + \chi_{4,1,0} + \chi_{2,1,3} + \chi_{2,1,5} + \chi_{2,1,2} + 2\chi_{0,1,2} \\
& + 2\chi_{0,1,5} + 2\chi_{0,3,2} + 2\chi_{0,3,5} + 2\chi_{0,2,4} + 2\chi_{0,2,1} + \chi_{0,4,2} + 2\chi_{0,4,3} + 2\chi_{0,4,0} \\
& + 2\chi_{0,5,0} + 2\chi_{0,5,1} + \chi_{0,4,5} + 2\chi_{0,5,4} + 2\chi_{0,5,3} + \chi_{2,0,1} + \chi_{2,0,2} + \chi_{2,0,5} \\
& + \chi_{2,0,4} + \chi_{2,1,0} \\
(6 - 2 - B - b) & \chi_{5,2,3} + 2\chi_{1,2,3} + 2\chi_{1,4,0} + 2\chi_{1,4,3} + \chi_{1,3,2} + \chi_{1,3,5} + 2\chi_{1,4,2} + 2\chi_{1,4,5} \\
& + \chi_{1,5,0} + \chi_{1,5,3} + \chi_{2,0,1} + \chi_{2,0,2} + \chi_{2,0,5} + \chi_{2,0,4} + \chi_{2,1,0} + \chi_{2,1,2}
\end{aligned}$$

$$\begin{aligned}
& +\chi_{2,1,3} + \chi_{2,1,5} + \chi_{2,3,1} + \chi_{2,3,4} + 2\chi_{2,5,0} + 2\chi_{2,5,3} + \chi_{3,0,2} + \chi_{3,1,0} \\
& +\chi_{3,0,5} + \chi_{3,1,3} + \chi_{3,1,2} + \chi_{3,1,5} + \chi_{3,2,0} + \chi_{3,2,3} + 2\chi_{1,0,5} + 2\chi_{1,0,2} \\
& +2\chi_{0,5,1} + 2\chi_{0,5,3} + \chi_{4,0,2} + 2\chi_{0,5,4} + \chi_{0,4,2} + 2\chi_{0,4,3} + 2\chi_{0,4,0} + \chi_{0,4,5} \\
& +2\chi_{0,5,0} + \chi_{4,0,5} + \chi_{4,1,2} + \chi_{4,1,5} + \chi_{4,2,0} + \chi_{4,1,0} + \chi_{4,1,3} + \chi_{4,2,3} \\
& +\chi_{5,0,2} + \chi_{5,1,3} + \chi_{5,1,2} + \chi_{5,1,5} + \chi_{5,2,0} + \chi_{5,1,0} + \chi_{5,0,5} + 2\chi_{1,2,0} \\
& +2\chi_{0,1,2} + 2\chi_{0,1,5} + 2\chi_{0,2,1} + 2\chi_{0,2,4} + 2\chi_{0,3,2} \\
(6 - 2 - B - c) \quad & 2\chi_{5,0,4} + 2\chi_{5,1,0} + \chi_{5,0,5} + \chi_{5,1,2} + \chi_{5,1,5} + 2\chi_{5,1,3} + \chi_{5,2,1} + \chi_{5,2,4} \\
& +\chi_{5,3,1} + \chi_{5,0,2} + 2\chi_{0,1,2} + 2\chi_{0,1,5} + 2\chi_{0,2,1} + 2\chi_{0,2,4} + 2\chi_{0,4,0} + 2\chi_{0,3,2} \\
& +2\chi_{0,3,5} + \chi_{0,4,5} + 2\chi_{0,5,0} + 2\chi_{0,4,3} + \chi_{0,4,2} + 2\chi_{0,5,1} + 2\chi_{0,5,3} + 2\chi_{0,5,4} \\
& +\chi_{1,0,2} + \chi_{1,0,1} + \chi_{1,0,5} + 2\chi_{1,0,4} + 2\chi_{1,2,0} + 2\chi_{1,2,3} + \chi_{1,2,4} + 2\chi_{1,3,1} \\
& +\chi_{1,4,2} + \chi_{1,4,5} + 2\chi_{1,5,1} + \chi_{2,0,1} + \chi_{2,0,4} + \chi_{2,0,2} + \chi_{2,0,5} + \chi_{2,1,0} \\
& +\chi_{2,1,3} + \chi_{2,1,2} + \chi_{2,1,5} + \chi_{2,3,1} + \chi_{2,3,4} + 2\chi_{2,5,0} + 2\chi_{2,5,3} + \chi_{3,0,2} \\
& +\chi_{3,0,1} + \chi_{3,0,5} + 2\chi_{3,0,4} + \chi_{3,1,0} + 2\chi_{3,1,2} + \chi_{3,1,3} + 2\chi_{3,2,0} + 2\chi_{3,1,5} \\
& +2\chi_{3,2,3} + 2\chi_{3,2,1} + \chi_{3,2,4} + 2\chi_{3,4,0} + \chi_{3,4,2} + 2\chi_{3,4,3} + \chi_{3,4,5} + \chi_{3,5,1} \\
& +\chi_{4,0,2} + \chi_{4,1,2} + \chi_{4,0,5} + \chi_{4,1,0} + \chi_{4,1,3} + \chi_{4,1,5} + \chi_{4,2,3} + \chi_{4,2,0}
\end{aligned}$$

Table 7.5 : Cocycle invariants of twist spun torus knots $\tau^k T(2, m)$

Torus links	k	Alexander ideals	Color quandles	Invariants
$T(2, 3)$	2	$(T + 1, 3)(\cong R_3)$	$Z^3(R_3, \mathbf{Z}_3)$	$3 + 6t (3 - 2 - A)$
				$3 + 6t^2$
	3	$(T^2 - T + 1, 2)$	$Z^3(\mathbf{Z}_2[T, T^{-1}]/(T^2 + T + 1), \mathbf{Z}_2)$	$10 + 6t (3 - 3 - A - a)$
				$8 + 8t (3 - 3 - A - b)$
	4	$(T + 1, 3)(\cong R_3)$	$Z^3(R_3, \mathbf{Z}_3)$	$3 + 6t^2, 3 + 6t (p)$
	5	(1)		
6	$(T^2 - T + 1)$	$Z^3(R_3, \mathbf{Z}_3)$	9 for any cocycle (p)	
			$Z^3(\mathbf{Z}_2[T, T^{-1}]/(T^2 + T + 1), \mathbf{Z}_2)$	4 for any cocycle (p)
$T(2, 4)$	2	$(T^2 - 1, 2T - 2)$	$Z^3(R_4, \mathbf{Z}_2)$	$12 + 4t (4 - 2 - A - a)$
				$8 + 8t (4 - 2 - A - b)$
			$Z^3(R_4, \mathbf{Z}_3)$	16
			$Z^3(\mathbf{Z}_2[T, T^{-1}]/(T^2 + 1), \mathbf{Z}_2)$	$12 + 4t (4 - 2 - B - a)$
				$8 + 8t (4 - 2 - B - b)$
	$Z^3(\mathbf{Z}_2[T, T^{-1}]/(T^2 + 1), \mathbf{Z}_3)$	16 for any cocycles		
3	(1)			
4	(Δ_4)			
$T(2, 5)$	2	$(T^2 - 1, 2T - 3)$	$Z^3(R_5, \mathbf{Z}_5)$	$5 + 10t + 10t^4 (5 - 2 - A)$
				$5 + 10t^2 + 10t^3$
	3	(1)		
	4	$(T + 1, 5)(\cong R_5)$	$Z^3(R_5, \mathbf{Z}_5)$	(p)
	5	$(\Delta_5, 2)$		
	6	$(T + 1, 5)(\cong R_5)$	$Z^3(R_5, \mathbf{Z}_5)$	(p)
	7	(1)		
	8	$(T^2 + 5, 2T - 3)$	$Z^3(R_5, \mathbf{Z}_5)$	(p)
	9	(1)		
10	$(T^2 - 1, 2T - 3)$	$Z^3(R_5, \mathbf{Z}_5)$	(p)	
$T(2, 6)$	2	$(T^2 - 1, 3T - 3)$	$Z^3(R_3, \mathbf{Z}_3)$	$3 + 6t (6 - 2 - A)$
				$3 + 6t^2$
			$Z^3(R_6, \mathbf{Z}_2)$	36 for any cocycle
				$Z^3(R_6, \mathbf{Z}_3)$
			$24 + 12t^2$	
			$12 + 24t (6 - 2 - B - b)$	
			$12 + 24t^2$	
	$12 + 12t + 12t^2 (6 - 2 - B - c)$			
	3	$(T^3 - 1)$	$Z^3(\mathbf{Z}_2[T, T^{-1}]/(T^2 + T + 1), \mathbf{Z}_2)$	16 for any cocycle
	4	$(T^2 - 1, 3T - 3)$	$Z^3(R_3, \mathbf{Z}_3)$	(p)
			$Z^3(R_6, \mathbf{Z}_2)$	(p)
			$Z^3(R_6, \mathbf{Z}_3)$	(p)
5	(1)			
6	(Δ_6)	$Z^3(R_6, \mathbf{Z}_3)$	(p)	
		$Z^3(\mathbf{Z}_2[T, T^{-1}]/(T^2 + T + 1), \mathbf{Z}_2)$	(p)	

8 Computations with Surface Braids

In this section, we use surface braid theory to provide computations for $\tau^2 T(2, m)$. Some of the results here coincide with those of the previous section, but there are advantages to the current approach that we outline. First, by making computations in more than one context, we are able to cross-check our results. Second, the braid chart provides a snap-shot of the entire knotted surface whereas in a movie description more work is needed to reconstruct the diagram of the knotting. Third, presentations for the fundamental quandle and the form of the partition function can be read directly from the braid chart. Thus the techniques we present for the current example are applicable in general to surfaces that are given in braid form.

We begin with a brief review of the theory of surface braids; see [25, 24, 7] for more details.

8.1 Definition. Let D^2 and D be 2-disks and X_m a fixed set of m interior points of D^2 . By $pr_1 : D^2 \times D \rightarrow D^2$ and $pr_2 : D^2 \times D \rightarrow D$, we mean the projections to the first factor and to the second factor.

A *surface braid* ([24], [39]) of degree m is a compact, oriented surface S properly embedded in $D^2 \times D$ such that the restriction of pr_2 to S is a degree- m simple branched covering map and $\partial S = X_m \times \partial D \subset D^2 \times \partial D$. A degree- m branched covering map $f : S \rightarrow D$ is *simple* if $|f^{-1}(y)| = m$ or $m - 1$ for $y \in D$. In this case, the branch points are simple ($z \mapsto z^2$).

A surface braid S of degree m is extended to a closed surface \widehat{S} in $D^2 \times S^2$ such that $\widehat{S} \cap (D^2 \times D) = S$ and $\widehat{S} \cap (D^2 \times \overline{D}) = X_m \times \overline{D}$, where S^2 is the 2-sphere obtained from D^2 by attaching a 2-disk \overline{D} along the boundary. By identifying $D^2 \times S^2$ with the tubular neighborhood of a standard 2-sphere in \mathbf{R}^4 , we assume that \widehat{S} is a closed oriented surface embedded in \mathbf{R}^4 . We call it the *closure* of S in \mathbf{R}^4 . It is proved in [25] that every closed oriented surface embedded in \mathbf{R}^4 is ambient isotopic to the closure of a surface braid.

Two surface braids S and S' in $D^2 \times D$ are said to be *equivalent* if there is an isotopy $\{h_t\}$ of $D^2 \times D$ such that

1. $h_0 = \text{id}$, $h_1(S) = S'$,
2. for each $t \in [0, 1]$, h_t is fiber-preserving; that is, there is a homeomorphism $\underline{h}_t : D \rightarrow D$ with $\underline{h}_t \circ pr_2 = pr_2 \circ h_t$, and
3. for each $t \in [0, 1]$, $h_t|_{D^2 \times \partial D} = \text{id}$.

Let C_m be the configuration space of unordered m interior points of D^2 . We identify the fundamental group $\pi_1(C_m, X_m)$ of C_m with base point X_m with the braid group B_m on m strings. Let S denote a surface braid and $\Sigma(S) \subset D$ the branch point set of the branched covering map $S \rightarrow D$. For a path $a : [0, 1] \rightarrow D - \Sigma(S)$, we define a path

$$\rho_S(a) : [0, 1] \rightarrow C_m$$

by

$$\rho_S(a)(t) = pr_1(S \cap (D^2 \times \{a(t)\})).$$

If $pr_1(S \cap (D^2 \times \{a(0)\})) = pr_1(S \cap (D^2 \times \{a(1)\})) = X_m$, then the path $\rho_S(a)$ represents an element of $\pi_1(C_m, X_m) = B_m$. Take a point y_0 in ∂D . The *braid monodromy* of S is the homomorphism

$$\rho_S : \pi_1(D - \Sigma(S), y_0) \rightarrow B_m$$

such that $\rho_S([a]) = [\rho_S(a)]$ for any loop a in $D - \Sigma(S)$ with base point y_0 .

8.2 Definition. Let $\Sigma(S) = \{y_1, \dots, y_n\}$. Take a regular neighborhood $N(\Sigma(S)) = N(y_1) \cup \dots \cup N(y_n)$ in D . A *Hurwitz arc system* $\mathcal{A} = (\alpha_1, \dots, \alpha_n)$ for $\Sigma(S)$ is an n -tuple of simple arcs in $E(\Sigma(S)) = \text{cl}(D \setminus N(\Sigma(S)))$ such that each α_i starts from a point of $\partial N(y_i)$ and ends at y_0 , and $\alpha_i \cap \alpha_j = \{y_0\}$ for $i \neq j$, and $\alpha_1, \dots, \alpha_n$ appear in this order around y_0 .

Let γ_i ($i = 1, \dots, n$) be the loop $\alpha_i^{-1} \cdot \partial N(y_i) \cdot \alpha_i$ in $D - \Sigma(S)$ with base point y_0 which goes along α_i , turns around the endpoint of α_i in the positive direction, and returns along α_i . The *braid system* of S associated with \mathcal{A} is an n -tuple of m -braids

$$(\rho_S([\gamma_1]), \rho_S([\gamma_2]), \dots, \rho_S([\gamma_n])).$$

8.3 Definition. An *m -chart* [24] is oriented, labelled graph Γ in D , which may be empty or have closed edges without vertices called *hoops*, satisfying the following conditions:

1. Every vertex has degree one, four or six.
2. The labels of edges are in $\{1, 2, \dots, m-1\}$.
3. For each degree-six vertex, three consecutive edges are oriented inward and the other three are outward, and these six edges are labelled i and $i+1$ alternately for some i .
4. For each degree-four vertex, diagonal edges have the same label and are oriented coherently, and the labels i and j of the diagonals satisfy $|i-j| > 1$.

We call a degree 1 (resp. degree 6) vertex a *black* (resp. *white*) vertex. A degree 4 vertex is called a *crossing point of the chart*.

For an m -chart Γ , we consider a surface braid S of degree m satisfying the following conditions:

1. For a regular neighborhood $N(\Gamma)$ of Γ in D and for any $y \in D - \text{int}N(\Gamma)$ the projection is $pr_1(S \cap (D^2 \times \{y\})) = X_m$, where X_m denotes the m fixed interior points of D^2 .
2. The branch point set of S coincides with the set of the black vertices of Γ .
3. For a path $\alpha : [0, 1] \rightarrow D$ which is in general position with respect to Γ and $\alpha(0), \alpha(1)$ are in $D - \text{int}N(\Gamma)$, the m -braid determined by $\rho_S(\alpha)$ is the m -braid presented by the intersection braid word $w_\Gamma(a)$.

Then we call S a *surface braid described by Γ* .

In general, the singularity set of the image of S by the projection $I_1 \times I_2 \times I_3 \times I_4 \rightarrow I_2 \times I_3 \times I_4$ is identified naturally with the chart Γ in the sense of [26] and [7]. The white vertices are in one-to-one correspondence to the triple points and the black vertices are to the branch points. Figure 17 shows the relationship schematically, see [26] and [7] for details.

Let m be an integer with $m \geq 3$ and let Γ be the 4-chart illustrated in Fig. 18. Let S be the surface braid of degree 4 described by Γ . The closure of S in R^4 is the surface link $\tau^2(T(2, m))$ which is obtained from $T(2, m)$, the torus knot/link of type $(2, m)$, by Zeeman's 2-twist spinning. (If m is odd, then it is a 2-knot. If m is even, then it consists of 2 components; one is a 2-sphere and the other is a torus. If $m = 0, 1$, or 2 , then $\tau^2(T(2, m))$ is a ribbon surface link and every quandle cocycle invariant of it is trivial. So we assume $m \geq 3$ in this paper.)

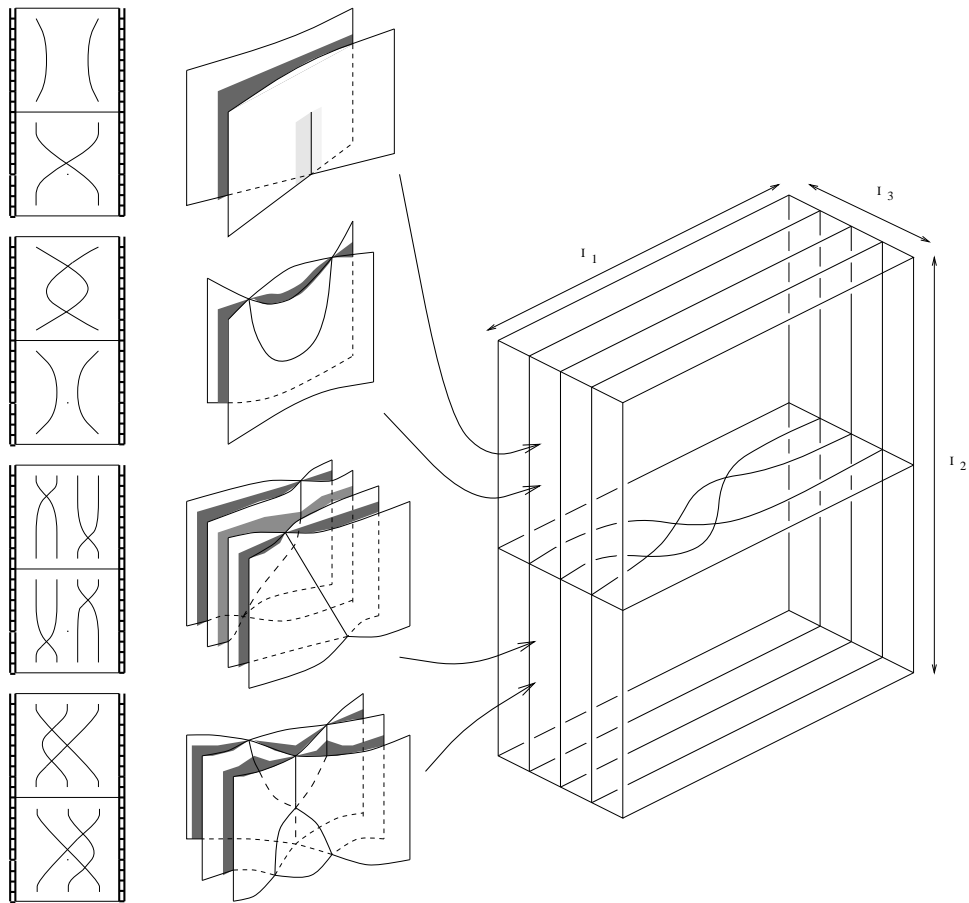


Figure 17: Projections and charts

8.4 Theorem. For a quandle 3-cocycle $\theta \in Z_Q^3(X; A)$, the state sum $\Phi_\theta(\tau^2(T(2, m)))$ is

$$\begin{aligned}
& \sum_{y_1, y_2} \prod_{j:\text{odd}; 1 \leq j \leq m-2} \theta(y_2 * (y_1 y_2)^{(j-1)/2} y_1^{-1}, y_1 * (y_2 y_1)^{(j+1)/2} y_1^{-2}, y_1)^{-1} \\
& \times \prod_{j:\text{even}; 1 \leq j \leq m-2} \theta(y_1 * (y_2 y_1)^{j/2} y_1^{-2}, y_2 * (y_1 y_2)^{j/2} y_1^{-1}, y_1)^{-1} \\
& \times \prod_{j:\text{odd}; 1 \leq j \leq m-1} \theta(y_1 * (y_2 y_1)^{(j-5)/2} y_2, y_2 * (y_1 y_2)^{(j-3)/2}, y_1 * y_2 y_1^{-1})^{-1} \\
& \times \prod_{j:\text{even}; 1 \leq j \leq m-1} \theta(y_2 * (y_1 y_2)^{(j-4)/2}, y_1 * (y_2 y_1)^{(j-4)/2} y_2, y_1 * y_2 y_1^{-1})^{-1} \\
& \times \prod_{j:\text{odd}; 1 \leq j \leq m-1} \theta(y_1 * y_2 y_1^{-1}, y_2 * (y_1 y_2)^{(j-3)/2}, y_1 * (y_2 y_1)^{(j-3)/2} y_2)^{+1} \\
& \times \prod_{j:\text{even}; 1 \leq j \leq m-1} \theta(y_1 * y_2 y_1^{-1}, y_1 * (y_2 y_1)^{(j-4)/2} y_2, y_2 * (y_1 y_2)^{(j-2)/2})^{+1} \\
& \times \prod_{j:\text{odd}; 1 \leq j \leq m-2} \theta(y_1, y_2 * (y_1 y_2)^{(j-1)/2}, y_1 * (y_2 y_1)^{(j-1)/2} y_2)^{+1} \\
& \times \prod_{j:\text{even}; 1 \leq j \leq m-2} \theta(y_1, y_1 * (y_2 y_1)^{(j-2)/2} y_2, y_2 * (y_1 y_2)^{j/2})^{+1},
\end{aligned}$$

where y_1, y_2 run over all elements of X satisfying $y_2 * (y_1 y_2)^{(m-1)/2} = y_1$ (if m is odd) or $y_1 * (y_2 y_1)^{m/2} = y_1$ (if m is even), and $y_1 * y_2^2 = y_1$.

The formula is restated as follows.

8.5 Theorem. Let $m = 2n + 1$ (resp. $m = 2n$). For a quandle 3-cocycle $\theta \in Z_Q^3(X; A)$, the state sum $\Phi_\theta(\tau^2(T(2, m)))$ is

$$\begin{aligned}
& \sum_{y_1, y_2} \prod_{k=1}^{n(\text{resp. } n-1)} \theta(y_2 * (y_1 y_2)^{k-1} y_1^{-1}, y_1 * (y_2 y_1)^k y_1^{-2}, y_1)^{-1} \\
& \times \prod_{k=1}^{n-1} \theta(y_1 * (y_2 y_1)^k y_1^{-2}, y_2 * (y_1 y_2)^k y_1^{-1}, y_1)^{-1} \\
& \times \prod_{k=1}^n \theta(y_1 * (y_2 y_1)^{k-3} y_2, y_2 * (y_1 y_2)^{k-2}, y_1 * y_2 y_1^{-1})^{-1} \\
& \times \prod_{k=1}^{n(\text{resp. } n-1)} \theta(y_2 * (y_1 y_2)^{k-2}, y_1 * (y_2 y_1)^{k-2} y_2, y_1 * y_2 y_1^{-1})^{-1} \\
& \times \prod_{k=1}^n \theta(y_1 * y_2 y_1^{-1}, y_2 * (y_1 y_2)^{k-2}, y_1 * (y_2 y_1)^{k-2} y_2)^{+1} \\
& \times \prod_{k=1}^{n(\text{resp. } n-1)} \theta(y_1 * y_2 y_1^{-1}, y_1 * (y_2 y_1)^{k-2} y_2, y_2 * (y_1 y_2)^{k-1})^{+1} \\
& \times \prod_{k=1}^{n(\text{resp. } n-1)} \theta(y_1, y_2 * (y_1 y_2)^{k-1}, y_1 * (y_2 y_1)^{k-1} y_2)^{+1}
\end{aligned}$$

$$\times \prod_{k=1}^{n-1} \theta(y_1, y_1 * (y_2 y_1)^{k-1} y_2, y_2 * (y_1 y_2)^k)^{+1},$$

where y_1, y_2 run over all elements of X satisfying $y_2 * (y_1 y_2)^n = y_1$ (resp. $y_1 * (y_2 y_1)^n = y_1$) and $y_1 * y_2^2 = y_1$.

Proof. For the Hurwitz arc system $(\alpha_1, \dots, \alpha_6)$ illustrated in Fig. 18, the braid system

$$(w_1^{-1} \sigma_{k_1}^{\epsilon_1} w_1, w_2^{-1} \sigma_{k_2}^{\epsilon_2} w_2, \dots, w_6^{-1} \sigma_{k_6}^{\epsilon_6} w_6)$$

of S is given by

$$\begin{aligned} w_1 &= \sigma_2^{-(m-2)} \sigma_3 \sigma_2, & \sigma_{k_1}^{\epsilon_1} &= \sigma_3, \\ w_2 &= \sigma_2^{-1} \sigma_3 \sigma_2, & \sigma_{k_2}^{\epsilon_2} &= \sigma_1^{-1}, \\ w_3 &= \sigma_1^{-(m-1)} \sigma_3 \sigma_2, & \sigma_{k_3}^{\epsilon_3} &= \sigma_2, \\ w_4 &= \sigma_1^{-1} \sigma_2, & \sigma_{k_4}^{\epsilon_4} &= \sigma_2^{-1}, \\ w_5 &= \sigma_2^{-(m-2)}, & \sigma_{k_5}^{\epsilon_5} &= \sigma_1, \\ w_6 &= \sigma_2^{-1}, & \sigma_{k_6}^{\epsilon_6} &= \sigma_3^{-1}. \end{aligned}$$

For arcs $\{\beta_{1,1}, \dots, \beta_{1,m-2}, \beta_{2,1}, \dots, \beta_{2,m-1}, \beta_{3,1}, \dots, \beta_{3,m-1}, \beta_{4,1}, \dots, \beta_{4,m-2}\}$ as in Fig. 19, the intersection word $w_\Gamma(\beta_{i,j})$ ($i \in \{1, 2, 3, 4\}$) are as follows (sgn means the sign of the white vertex $W_{i,j}$ near the starting point of $\beta_{i,j}$, and labels mean the labels around $W_{i,j}$):

$$\begin{aligned} w_\Gamma(\beta_{1,j}) &= \sigma_2^{-(j-1)} \sigma_3 \sigma_2, & \text{sgn} &= -1, & \text{labels} &= \{2, 3\}, & (j &= 1, \dots, m-2); \\ w_\Gamma(\beta_{2,j}) &= \sigma_1^{-(j-1)} \sigma_3 \sigma_2, & \text{sgn} &= -1, & \text{labels} &= \{1, 2\}, & (j &= 1, \dots, m-1); \\ w_\Gamma(\beta_{3,j}) &= \sigma_2^{-(j-2)}, & \text{sgn} &= +1, & \text{labels} &= \{1, 2\}, & (j &= 1, \dots, m-1); \\ w_\Gamma(\beta_{4,j}) &= \sigma_3^{-(j-1)}, & \text{sgn} &= +1, & \text{labels} &= \{2, 3\}, & (j &= 1, \dots, m-2); \end{aligned}$$

Suppose that m is odd. Then the quandle automorphisms $Q(w_i)$ ($i = 1, \dots, 6$) of $F_Q\langle x_1, \dots, x_4 \rangle$ are as follows:

$$\begin{aligned} Q(\sigma_2^{-(m-2)} \sigma_3 \sigma_2) &: \begin{cases} x_1 \rightarrow x_1, \\ x_2 \rightarrow x_4 * (x_3 x_4)^{(m-3)/2} x_2^{-1}, \\ x_3 \rightarrow x_3 * (x_4 x_3)^{(m-3)/2} x_4 x_2^{-1}, \\ x_4 \rightarrow x_2, \end{cases} \\ Q(\sigma_2^{-1} \sigma_3 \sigma_2) &: \begin{cases} x_1 \rightarrow x_1, \\ x_2 \rightarrow x_4 * x_2^{-1}, \\ x_3 \rightarrow x_3 * x_4 x_2^{-1}, \\ x_4 \rightarrow x_2, \end{cases} \\ Q(\sigma_1^{-(m-1)} \sigma_3 \sigma_2) &: \begin{cases} x_1 \rightarrow x_1 * (x_2 x_3 x_2^{-1} x_1)^{(m-3)/2} x_2 x_3 x_2^{-1}, \\ x_2 \rightarrow x_3 * (x_2^{-1} x_1 x_2 x_3)^{(m-1)/2} x_2^{-1}, \\ x_3 \rightarrow x_4 * x_2^{-1}, \\ x_4 \rightarrow x_2, \end{cases} \\ Q(\sigma_1^{-1} \sigma_2) &: \begin{cases} x_1 \rightarrow x_3 * x_2^{-1}, \\ x_2 \rightarrow x_1 * x_2 x_3 x_2^{-1}, \\ x_3 \rightarrow x_2, \\ x_4 \rightarrow x_4, \end{cases} \end{aligned}$$

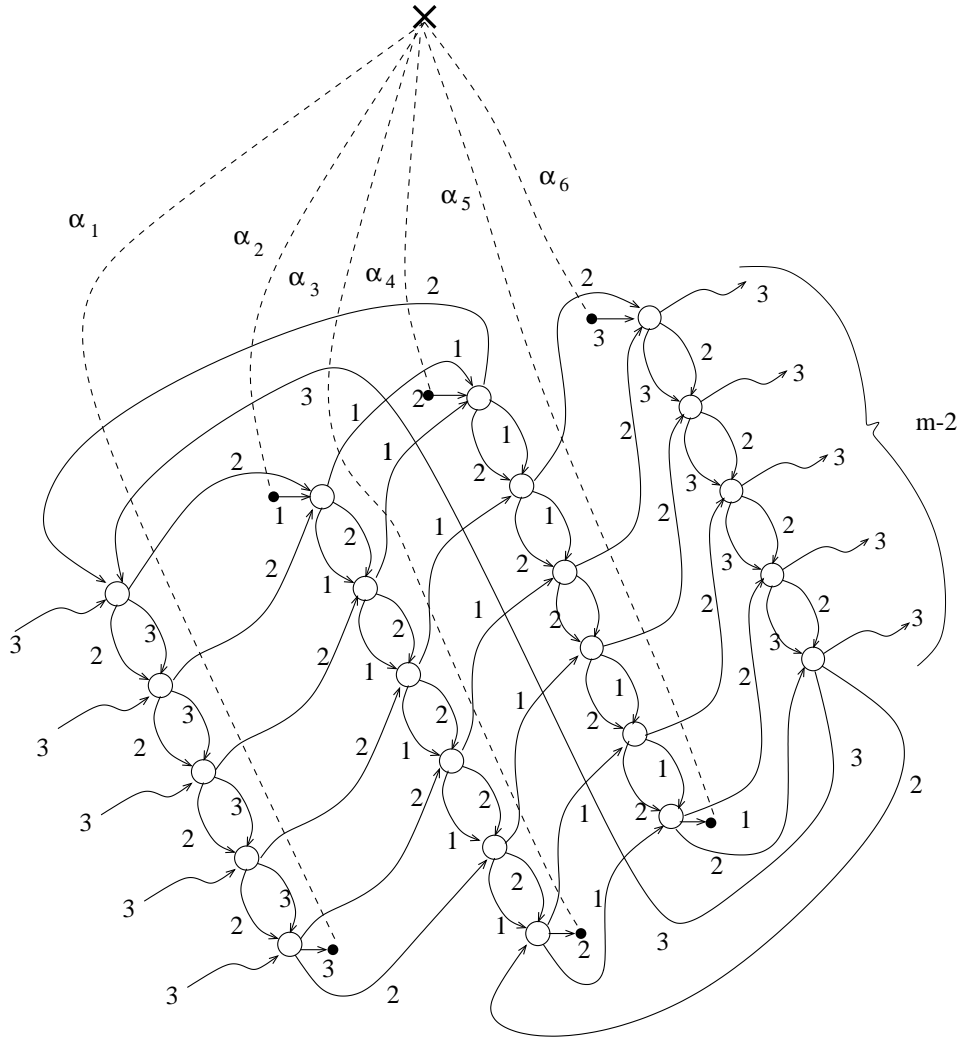


Figure 18: A braid chart and Hurwitz system for the 2-twist spun $T(2, m)$: Here $m = 7$

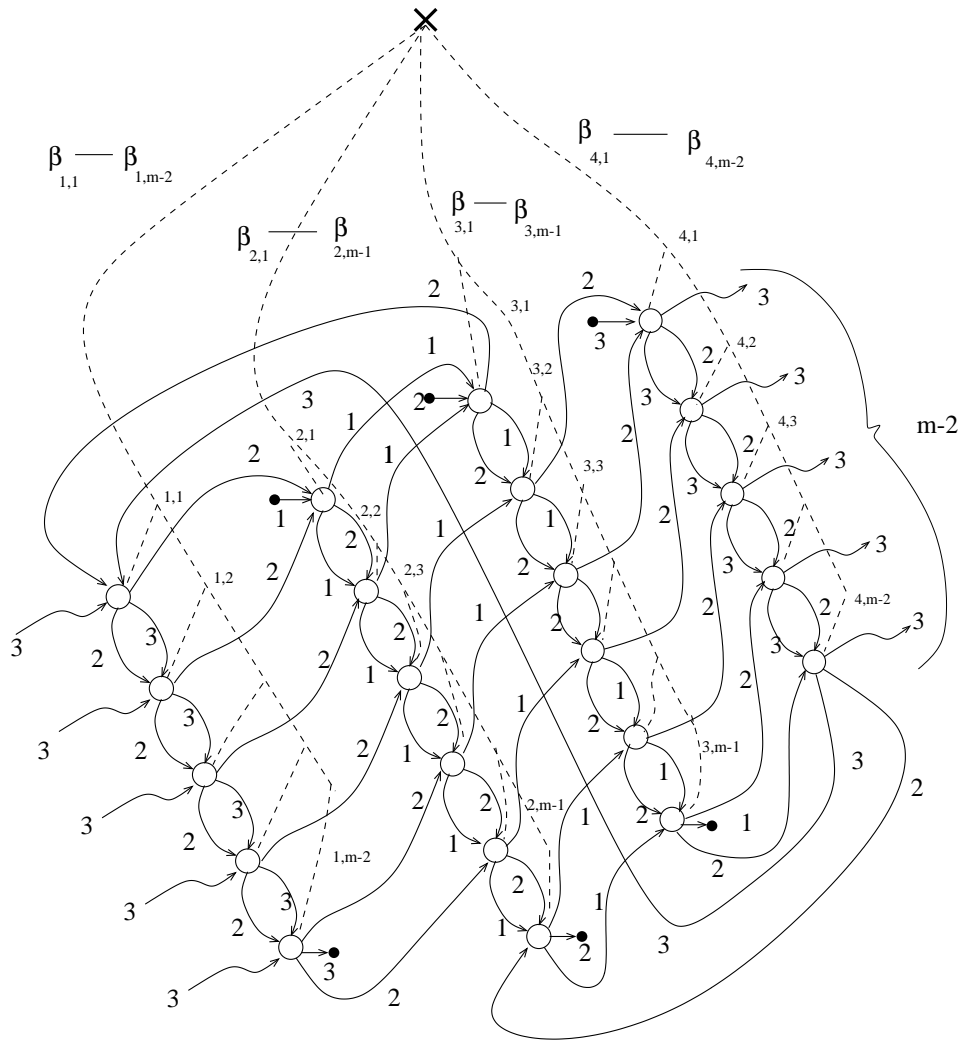


Figure 19: Paths to the preferred regions near triple points

$$Q(\sigma_2^{-(m-2)}) : \begin{cases} x_1 \rightarrow x_1, \\ x_2 \rightarrow x_3 * (x_2x_3)^{(m-3)/2}, \\ x_3 \rightarrow x_2 * (x_3x_2)^{(m-3)/2}x_3, \\ x_4 \rightarrow x_4, \end{cases}$$

$$Q(\sigma_2^{-1}) : \begin{cases} x_1 \rightarrow x_1, \\ x_2 \rightarrow x_3, \\ x_3 \rightarrow x_2 * x_3, \\ x_4 \rightarrow x_4, \end{cases}$$

Hence the defining relations $Q(w_i)(x_{k_i}) = Q(w_i)(x_{k_i+1})$ ($i = 1, \dots, 6$) of $Q(S)$ are

$$\begin{aligned} x_3 * (x_4x_3)^{(m-3)/2}x_4x_2^{-1} &= x_2, \\ x_1 &= x_4 * x_2^{-1}, \\ x_3 * (x_2^{-1}x_1x_2x_3)^{(m-1)/2}x_2^{-1} &= x_4 * x_2^{-1}, \\ x_1 * x_2x_3x_2^{-1} &= x_2, \\ x_1 &= x_3 * (x_2x_3)^{(m-3)/2}, \\ x_2 * x_3 &= x_4. \end{aligned}$$

Thus the quandle $Q(S)$, for odd m , is

$$\begin{aligned} \langle x_1, \dots, x_4 \mid & x_3 * (x_2x_3)^{(m-1)/2} = x_2, \\ & x_2 * x_3^2 = x_2, \\ & x_1 = x_2 * x_3x_2^{-1}, \\ & x_4 = x_2 * x_3 \rangle \\ = \langle x_2, x_3 \mid & x_3 * (x_2x_3)^{(m-1)/2} = x_2, \\ & x_2 * x_3^2 = x_2 \rangle. \end{aligned}$$

This is isomorphic to the dihedral quandle R_m .

Suppose that m is even. Then the quandle automorphisms $Q(w_i)$ ($i = 1, \dots, 6$) of $F_Q\langle x_1, \dots, x_4 \rangle$ are as follows:

$$Q(\sigma_2^{-(m-2)}\sigma_3\sigma_2) : \begin{cases} x_1 \rightarrow x_1, \\ x_2 \rightarrow x_3 * (x_4x_3)^{(m-4)/2}x_4x_2^{-1}, \\ x_3 \rightarrow x_4 * (x_3x_4)^{(m-2)/2}x_2^{-1}, \\ x_4 \rightarrow x_2, \end{cases}$$

$$Q(\sigma_2^{-1}\sigma_3\sigma_2) : \begin{cases} x_1 \rightarrow x_1, \\ x_2 \rightarrow x_4 * x_2^{-1}, \\ x_3 \rightarrow x_3 * x_4x_2^{-1}, \\ x_4 \rightarrow x_2, \end{cases}$$

$$Q(\sigma_1^{-(m-1)}\sigma_3\sigma_2) : \begin{cases} x_1 \rightarrow x_3 * (x_2^{-1}x_1x_2x_3)^{(m-2)/2}x_2^{-1}, \\ x_2 \rightarrow x_1 * (x_2x_3x_2^{-1}x_1)^{(m-2)/2}x_2x_3x_2^{-1}, \\ x_3 \rightarrow x_4 * x_2^{-1}, \\ x_4 \rightarrow x_2, \end{cases}$$

$$\begin{aligned}
Q(\sigma_1^{-1}\sigma_2) &: \begin{cases} x_1 \rightarrow x_3 * x_2^{-1}, \\ x_2 \rightarrow x_1 * x_2 x_3 x_2^{-1}, \\ x_3 \rightarrow x_2, \\ x_4 \rightarrow x_4, \end{cases} \\
Q(\sigma_2^{-(m-2)}) &: \begin{cases} x_1 \rightarrow x_1, \\ x_2 \rightarrow x_2 * (x_3 x_2)^{(m-4)/2} x_3, \\ x_3 \rightarrow x_3 * (x_2 x_3)^{(m-2)/2}, \\ x_4 \rightarrow x_4, \end{cases} \\
Q(\sigma_2^{-1}) &: \begin{cases} x_1 \rightarrow x_1, \\ x_2 \rightarrow x_3, \\ x_3 \rightarrow x_2 * x_3, \\ x_4 \rightarrow x_4, \end{cases}
\end{aligned}$$

Hence the defining relations $Q(w_i)(x_{k_i}) = Q(w_i)(x_{k_i+1})$ ($i = 1, \dots, 6$) of $Q(S)$ are

$$\begin{aligned}
x_4 * (x_3 x_4)^{(m-2)/2} x_2^{-1} &= x_2, \\
x_1 &= x_4 * x_2^{-1}, \\
x_1 * (x_2 x_3 x_2^{-1} x_1)^{(m-2)/2} x_2 x_3 x_2^{-1} &= x_4 * x_2^{-1}, \\
x_1 * x_2 x_3 x_2^{-1} &= x_2, \\
x_1 &= x_2 * (x_3 x_2)^{(m-4)/2} x_3, \\
x_2 * x_3 &= x_4.
\end{aligned}$$

Thus the quandle $Q(S)$, for even m , is

$$\begin{aligned}
\langle x_1, \dots, x_4 \mid & \begin{aligned} &x_2 * (x_3 x_2)^{m/2} = x_2, \\ &x_2 * x_3^2 = x_2, \\ &x_1 = x_2 * x_3 x_2^{-1}, \\ &x_4 = x_2 * x_3 \end{aligned} \\ &= \langle x_2, x_3 \mid & \begin{aligned} &x_2 * (x_3 x_2)^{m/2} = x_2, \\ &x_2 * x_3^2 = x_2 \end{aligned} \rangle.
\end{aligned}$$

Now we calculate the Boltzmann weight for each white vertex. Let $\iota : \langle x_1, x_2, x_3, x_4 \rangle \rightarrow Q(S)$ be the natural projection map (that is i_* in [4]). Let θ be a quandle 3-cocycle of a finite quandle, and c a coloring.

1. $w_\Gamma(\beta_{1,j}) = \sigma_2^{-(j-1)} \sigma_3 \sigma_2$, $\text{sgn} = -1$, labels = $\{2, 3\}$, ($j = 1, \dots, m-2$).

(a) For odd j ($1 \leq j \leq m-2$), the composition of $Q(\sigma_2^{-(j-1)} \sigma_3 \sigma_2)$ and ι maps

$$\begin{cases} x_1 \rightarrow x_1 & \rightarrow x_2 * x_3 x_2^{-1} \\ x_2 \rightarrow x_3 * (x_4 x_3)^{(j-3)/2} x_4 x_2^{-1} & \rightarrow x_3 * (x_2 x_3)^{(j-1)/2} x_2^{-1} \\ x_3 \rightarrow x_4 * (x_3 x_4)^{(j-1)/2} x_2^{-1} & \rightarrow x_2 * (x_3 x_2)^{(j+1)/2} x_2^{-2} \\ x_4 \rightarrow x_2 & \rightarrow x_2. \end{cases}$$

Hence the Boltzmann weight is

$$B = \theta(c(x_3 * (x_2x_3)^{(j-1)/2}x_2^{-1}), c(x_2 * (x_3x_2)^{(j+1)/2}x_2^{-2}), c(x_2))^{-1}.$$

Put $j = 2k - 1$, then

$$B = \theta(c(x_3 * (x_2x_3)^{k-1}x_2^{-1}), c(x_2 * (x_3x_2)^kx_2^{-2}), c(x_2))^{-1},$$

where $k = 1, 2, \dots, n$ if $m = 2n + 1$, or $k = 1, 2, \dots, n - 1$ if $m = 2n$.

(b) For even j ($1 \leq j \leq m - 2$), the composition of $Q(\sigma_2^{-(j-1)}\sigma_3\sigma_2)$ and ι maps

$$\begin{cases} x_1 & \rightarrow x_1 & \rightarrow x_2 * x_3x_2^{-1} \\ x_2 & \rightarrow x_4 * (x_3x_4)^{(j-2)/2}x_2^{-1} & \rightarrow x_2 * (x_3x_2)^{j/2}x_2^{-1} \\ x_3 & \rightarrow x_3 * (x_4x_3)^{(j-2)/2}x_4x_2^{-1} & \rightarrow x_3 * (x_2x_3)^{j/2}x_2^{-1} \\ x_4 & \rightarrow x_2 & \rightarrow x_2. \end{cases}$$

Hence the Boltzmann weight is

$$B = \theta(c(x_2 * (x_3x_2)^{j/2}x_2^{-2}), c(x_3 * (x_2x_3)^{j/2}x_2^{-1}), c(x_2))^{-1}.$$

Put $j = 2k$, then

$$B = \theta(c(x_2 * (x_3x_2)^kx_2^{-2}), c(x_3 * (x_2x_3)^kx_2^{-1}), c(x_2))^{-1},$$

where $k = 1, 2, \dots, n - 1$.

2. $w_\Gamma(\beta_{2,j}) = \sigma_1^{-(j-1)}\sigma_3\sigma_2$, $\text{sgn} = -1$, labels = $\{1, 2\}$, ($j = 1, \dots, m - 1$).

(a) For odd j ($1 \leq j \leq m - 1$), the composition of $Q(\sigma_1^{-(j-1)}\sigma_3\sigma_2)$ and ι maps

$$\begin{cases} x_1 & \rightarrow x_1 * (x_2x_3x_2^{-1}x_1)^{(j-1)/2}x_1^{-1} & \rightarrow x_2 * (x_3x_2)^{(j-5)/2}x_3 \\ x_2 & \rightarrow x_3 * (x_2^{-1}x_1x_2x_3)^{(j-1)/2}x_2^{-1} & \rightarrow x_3 * (x_2x_3)^{(j-3)/2} \\ x_3 & \rightarrow x_4 * x_2^{-1} & \rightarrow x_2 * x_3x_2^{-1} \\ x_4 & \rightarrow x_2 & \rightarrow x_2. \end{cases}$$

Hence the Boltzmann weight is

$$B = \theta(c(x_2 * (x_3x_2)^{(j-5)/2}x_3), c(x_3 * (x_2x_3)^{(j-3)/2}), c(x_2 * x_3x_2^{-1}))^{-1}.$$

Put $j = 2k - 1$, then

$$B = \theta(c(x_2 * (x_3x_2)^{k-3}x_3), c(x_3 * (x_2x_3)^{k-2}), c(x_2 * x_3x_2^{-1}))^{-1},$$

where $k = 1, 2, \dots, n$.

(b) For even j ($1 \leq j \leq m-1$), the composition of $Q(\sigma_1^{-(j-1)}\sigma_3\sigma_2)$ and ι maps

$$\begin{cases} x_1 & \rightarrow x_3 * (x_2^{-1}x_1x_2x_3)^{(j-2)/2}x_2^{-1} & \rightarrow x_3 * (x_2x_3)^{(j-4)/2} \\ x_2 & \rightarrow x_1 * (x_2x_3x_2^{-1}x_1)^{j/2}x_1^{-1} & \rightarrow x_2 * (x_3x_2)^{(j-4)/2}x_3 \\ x_3 & \rightarrow x_4 * x_2^{-1} & \rightarrow x_2 * x_3x_2^{-1} \\ x_4 & \rightarrow x_2 & \rightarrow x_2. \end{cases}$$

Hence the Boltzmann weight is

$$B = \theta(c(x_3 * (x_2x_3)^{(j-4)/2}), c(x_2 * (x_3x_2)^{(j-4)/2}x_3), c(x_2 * x_3x_2^{-1}))^{-1}.$$

Put $j = 2k$, then

$$B = \theta(c(x_3 * (x_2x_3)^{k-2}), c(x_2 * (x_3x_2)^{k-2}x_3), c(x_2 * x_3x_2^{-1}))^{-1},$$

where $k = 1, 2, \dots, n$ if $m = 2n + 1$, $k = 1, 2, \dots, n-1$ if $m = 2n$.

3. $w_\Gamma(\beta_{3,j}) = \sigma_2^{-(j-2)}$, $\text{sgn} = +1$, labels = $\{1, 2\}$, ($j = 1, \dots, m-1$).

(a) For odd j ($1 \leq j \leq m-1$), the composition of $Q(\sigma_2^{-(j-2)})$ and ι maps

$$\begin{cases} x_1 & \rightarrow x_1 & \rightarrow x_2 * x_3x_2^{-1} \\ x_2 & \rightarrow x_3 * (x_2x_3)^{(j-3)/2} & \rightarrow x_3 * (x_2x_3)^{(j-3)/2} \\ x_3 & \rightarrow x_2 * (x_3x_2)^{(j-3)/2}x_3 & \rightarrow x_2 * (x_3x_2)^{(j-3)/2}x_3 \\ x_4 & \rightarrow x_4 & \rightarrow x_2 * x_3. \end{cases}$$

Hence the Boltzmann weight is

$$B = \theta(c(x_2 * x_3x_2^{-1}), c(x_3 * (x_2x_3)^{(j-3)/2}), c(x_2 * (x_3x_2)^{(j-3)/2}x_3))^{+1}.$$

Put $j = 2k - 1$, then

$$B = \theta(c(x_2 * x_3x_2^{-1}), c(x_3 * (x_2x_3)^{k-2}), c(x_2 * (x_3x_2)^{k-2}x_3))^{+1},$$

where $k = 1, 2, \dots, n$.

(b) For even j ($1 \leq j \leq m-1$), the composition of $Q(\sigma_2^{-(j-2)})$ and ι maps

$$\begin{cases} x_1 & \rightarrow x_1 & \rightarrow x_2 * x_3x_2^{-1} \\ x_2 & \rightarrow x_2 * (x_3x_2)^{(j-4)/2}x_3 & \rightarrow x_2 * (x_3x_2)^{(j-4)/2}x_3 \\ x_3 & \rightarrow x_3 * (x_2x_3)^{(j-2)/2} & \rightarrow x_3 * (x_2x_3)^{(j-2)/2} \\ x_4 & \rightarrow x_4 & \rightarrow x_2 * x_3. \end{cases}$$

Hence the Boltzmann weight is

$$B = \theta(c(x_2 * x_3x_2^{-1}), c(x_2 * (x_3x_2)^{(j-4)/2}x_3), c(x_3 * (x_2x_3)^{(j-2)/2}))^{+1}.$$

Put $j = 2k$, then

$$B = \theta(c(x_2 * x_3x_2^{-1}), c(x_2 * (x_3x_2)^{k-2}x_3), c(x_3 * (x_2x_3)^{k-1}))^{+1},$$

where $k = 1, 2, \dots, n$ if $m = 2n + 1$, $k = 1, 2, \dots, n-1$ if $m = 2n$.

4. $w_\Gamma(\beta_{4,j}) = \sigma_3^{-(j-1)}$, $\text{sgn} = +1$, labels = $\{2, 3\}$, ($j = 1, \dots, m-2$).

(a) For odd j ($1 \leq j \leq m-2$), the composition of $Q(\sigma_3^{-(j-1)})$ and ι maps

$$\begin{cases} x_1 & \rightarrow x_1 & \rightarrow x_2 * x_3 x_2^{-1} \\ x_2 & \rightarrow x_2 & \rightarrow x_2 \\ x_3 & \rightarrow x_3 * (x_4 x_3)^{(j-3)/2} x_4 & \rightarrow x_3 * (x_2 x_3)^{(j-1)/2} \\ x_4 & \rightarrow x_4 * (x_3 x_4)^{(j-1)/2} & \rightarrow x_2 * (x_3 x_2)^{(j-1)/2} x_3. \end{cases}$$

Hence the Boltzmann weight is

$$B = \theta(c(x_2), c(x_3 * (x_2 x_3)^{(j-1)/2}), c(x_2 * (x_3 x_2)^{(j-1)/2} x_3))^{+1}.$$

Put $j = 2k - 1$, then

$$B = \theta(c(x_2), c(x_3 * (x_2 x_3)^{k-1}), c(x_2 * (x_3 x_2)^{k-1} x_3))^{+1},$$

where $k = 1, 2, \dots, n$ if $m = 2n + 1$, $k = 1, 2, \dots, n - 1$ if $m = 2n$.

(b) For even j ($1 \leq j \leq m-2$), the composition of $Q(\sigma_3^{-(j-1)})$ and ι maps

$$\begin{cases} x_1 & \rightarrow x_1 & \rightarrow x_2 * x_3 x_2^{-1} \\ x_2 & \rightarrow x_2 & \rightarrow x_2 \\ x_3 & \rightarrow x_4 * (x_3 x_4)^{(j-2)/2} & \rightarrow x_2 * (x_3 x_2)^{(j-2)/2} x_3 \\ x_4 & \rightarrow x_3 * (x_4 x_3)^{(j-2)/2} x_4 & \rightarrow x_3 * (x_2 x_3)^{j/2}. \end{cases}$$

Hence the Boltzmann weight is

$$B = \theta(c(x_2), c(x_2 * (x_3 x_2)^{(j-2)/2} x_3), c(x_3 * (x_2 x_3)^{j/2}))^{+1}.$$

Put $j = 2k$, then

$$B = \theta(c(x_2), c(x_2 * (x_3 x_2)^{k-1} x_3), c(x_3 * (x_2 x_3)^k))^{+1},$$

where $k = 1, 2, \dots, n - 1$.

By replacing $c(x_2)$ and $c(x_3)$ by y_1 and y_2 , we have the theorem. \square

8.6 Examples. The case of $m = 3$ ($n = 1$)

$$\begin{aligned} & \sum_{y_1, y_2} \theta(y_2 * y_1, y_2, y_1)^{-1} \\ & \quad \times \theta(y_2, y_2 * y_1, y_2)^{-1} \\ & \quad \times \theta(y_2 * y_1, y_1, y_2)^{-1} \\ & \quad \times \theta(y_2, y_2 * y_1, y_1)^{+1} \\ & \quad \times \theta(y_2, y_1, y_2)^{+1} \\ & \quad \times \theta(y_1, y_2, y_1 * y_2)^{+1}, \end{aligned}$$

where y_1, y_2 run over all elements of X satisfying $y_2 * y_1 y_2 = y_1$ and $y_1 * y_2^2 = y_1$.

Put $z_1 = y_1 * y_2 = y_2 * y_1$ and $z_2 = y_1$ (and $z_1 * z_2 = y_2$), then

$$\begin{aligned} & \sum_{y_1, y_2} \theta(z_1, z_1 * z_2, z_2)^{-1} \\ & \quad \times \theta(z_1 * z_2, z_1, z_1 * z_2)^{-1} \\ & \quad \times \theta(z_1, z_2, z_1 * z_2)^{-1} \\ & \quad \times \theta(z_1 * z_2, z_1, z_2)^{+1} \\ & \quad \times \theta(z_1 * z_2, z_2, z_1 * z_2)^{+1} \\ & \quad \times \theta(z_2, z_1 * z_2, z_1)^{+1}, \end{aligned}$$

where z_1, z_2 run over all elements of X satisfying $z_2 * z_1 z_2 = z_1$ and $z_1 * z_2^2 = z_1$. This formula is the same as that in [4].

The case of $m = 4$ ($n = 2$)

$$\begin{aligned} & \sum_{y_1, y_2} \theta(y_2 * y_1^{-1}, y_1 * y_2, y_1)^{-1} \\ & \quad \times \theta(y_1 * y_2, y_2 * y_1 y_2 y_1^{-1}, y_1)^{-1} \\ & \quad \times \theta(y_1 * y_2, y_2 * y_1^{-1}, y_1 * y_2)^{-1} \\ & \quad \times \theta(y_1, y_2, y_1 * y_2)^{-1} \\ & \quad \times \theta(y_2 * y_1^{-1}, y_1, y_1 * y_2)^{-1} \\ & \quad \times \theta(y_1 * y_2, y_2 * y_1^{-1}, y_1)^{+1} \\ & \quad \times \theta(y_1 * y_2, y_2, y_1 * y_2)^{+1} \\ & \quad \times \theta(y_1 * y_2, y_1, y_2)^{+1} \\ & \quad \times \theta(y_1, y_2, y_1 * y_2)^{+1} \\ & \quad \times \theta(y_1, y_1 * y_2, y_2 * y_1 y_2)^{+1}, \end{aligned}$$

where y_1, y_2 run over all elements of X satisfying $y_1 * (y_2 y_1)^2 = y_1$ and $y_1 * y_2^2 = y_1$.

Notice that $y_1 * y_2 y_1^{-1} = y_1 * y_2^{-1} = y_1 * y_2$ and $y_1 * (y_2 y_1)^{-1} = y_1 * y_2 y_1$.

The case of $m = 5$ ($n = 2$)

$$\begin{aligned} & \sum_{y_1, y_2} \theta(y_2 * y_1, y_1 * y_2 y_1, y_1)^{-1} \\ & \quad \times \theta(y_1 * y_2, y_2, y_1)^{-1} \\ & \quad \times \theta(y_1 * y_2 y_1, y_1 * y_2, y_1)^{-1} \\ & \quad \times \theta(y_1 * y_2 y_1, y_2 * y_1, y_1 * y_2 y_1)^{-1} \\ & \quad \times \theta(y_1, y_2, y_1 * y_2 y_1)^{-1} \\ & \quad \times \theta(y_2 * y_1, y_1, y_1 * y_2 y_1)^{-1} \\ & \quad \times \theta(y_2, y_1 * y_2, y_1 * y_2 y_1)^{-1} \\ & \quad \times \theta(y_1 * y_2 y_1, y_2 * y_1, y_1)^{+1} \end{aligned}$$

$$\begin{aligned}
& \times \theta(y_1 * y_2 y_1, y_2, y_1 * y_2)^{+1} \\
& \times \theta(y_1 * y_2 y_1, y_1, y_2)^{+1} \\
& \times \theta(y_1 * y_2 y_1, y_1 * y_2, y_1 * y_2 y_1)^{+1} \\
& \times \theta(y_1, y_2, y_1 * y_2)^{+1} \\
& \times \theta(y_1, y_1 * y_2 y_1, y_2 * y_1)^{+1} \\
& \times \theta(y_1, y_1 * y_2, y_1 * y_2 y_1)^{+1},
\end{aligned}$$

where y_1, y_2 run over all elements of X satisfying $y_2 * (y_1 y_2)^2 = y_1$ and $y_1 * y_2^2 = y_1$.

8.7 Remark. The values of the partition function that we computed in this section differ from those in the preceding section. For example, using the dihedral quandle R_3 for the 2-twist-spun trefoil would result in $3 + 6t^2$ here for $(3 - 2 - A)$. This is because the orientations chosen are opposite.

Even if the same orientation is chosen, the state-sum expressions (before evaluation with specific cocycles) would be different. The expressions depend on the choice of diagram, and we used different diagrams based on different methods. The different expressions are related by coboundaries, that correspond to Roseman moves relating the two diagrams.

9 Symmetry and Cocycle Invariants

In this section, we discuss how the partition function behaves under mirror images and change of orientation.

For an element $\sum a_i g_i$ of a group ring $\mathbf{Z}[A]$ (where $a_i \in \mathbf{Z}$ and $g_i \in A$), we denote by $\overline{\sum a_i g_i}$ the element $\sum a_i g_i^{-1}$ in the group ring.

For a link L , we denote by $-L$ the same link with the opposite orientation, by L^* the mirror image of L .

9.1 Theorem. *For any link L and any quandle 2-cocycle $\phi \in Z^2(Q; A)$,*

$$\Phi_\phi(-L^*) = \overline{\Phi_\phi(L)}.$$

Proof. Let D be a link diagram of L . We may assume that the arcs of D around each crossing point are oriented downward as in Fig. 5. Let D^* be the link diagram which is obtained from D by reversing the vertical direction, and $-D^*$ the link diagram obtained from D^* by reversing the orientation of the arcs of D^* . Obviously, the diagram $-D^*$ presents the link $-L^*$. Each positive (negative, resp.) crossing of D , which looks the left (right) side of Fig. 5, changes to a negative (positive) crossing of $-D^*$, which looks the right (left) side of Fig. 5. We notice that the labels $x, y, x * y$ around the crossing point of D are inherited to the corresponding crossing of $-D^*$. So the colorings of D by a quandle Q are naturally in one-to-one correspondence to the colorings of $-D^*$, and if the Boltzmann weight is $\phi(x, y)^\epsilon$, then the corresponding crossing point has Boltzmann weight $\phi(x, y)^{-\epsilon}$. Therefore we have $\Phi_\phi(-L^*) = \overline{\Phi_\phi(L)}$. \square

For a surface link F , we denote by $-F$ the same surface link with the opposite orientation, by F^* the mirror image of F .

9.2 Theorem. For any surface link F and any quandle 3-cocycle $\theta \in Z^3(Q; A)$,

$$\Phi_\theta(-F^*) = \overline{\Phi_\theta(F)}.$$

Proof. The proof is similar to the classical case. Let D be a broken surface diagram of F . We may assume that every triple point of D looks like one of Fig. 9 in a movie. Let D^* be the diagram which is obtained from D by reversing the vertical direction in each cross-section of the movie, and $-D^*$ the link diagram obtained from D^* by reversing the orientation of the arcs of each cross-sectional link diagram of D^* . Obviously, the diagram $-D^*$ presents the surface link $-F^*$. Each positive (negative, resp) triple point of D , which looks like one of Fig. 9, changes to a negative (positive) crossing of $-D^*$, which looks like another of the figure. For example, a triple point looking like the (1,1)-entry of Fig. 9 changes to one like the (1,6)-entry. A triple point looking like (2,2)-entry of Fig. 9 changes to one like (5,3)-entry, etc. We notice that the labels p, q, r around the crossing point of D indicated in Fig. 9 are inherited to the corresponding crossing of $-D^*$. So the colorings of D by a quandle Q are naturally in one-to-one correspondence to the colorings of $-D^*$, and if the Boltzmann weight is $\theta(p, q, r)^\epsilon$, then the corresponding crossing point has Boltzmann weight $\theta(p, q, r)^{-\epsilon}$. Therefore we have $\Phi_\theta(-F^*) = \overline{\Phi_\theta(F)}$. \square

9.3 Example. The surface link $\tau^2(T(2, m))$ is isotopic to its mirror image $\tau^2(T(2, m))^*$. (This is well-known for the case that m is an odd integer, and studied in more general cases, cf. [31].) Hence

$$\Phi_\theta(\tau^2(T(2, m))) = \Phi_\theta(\tau^2(T(2, m))^*) = \overline{\Phi_\theta(-\tau^2(T(2, m)))} = \overline{\Phi_\theta(-\tau^2(T(2, m))^*)}.$$

Thus, if we know $\Phi_\theta(\tau^2(T(2, m)))$, we do not need to calculate the invariants of $-\tau^2(T(2, m))$, $\tau^2(T(2, m))^*$ and $-\tau^2(T(2, m))^*$.

References

- [1] Baez, J. C.; Langford, L., *2-tangles*, Lett. Math. Phys. 43 (1998), no. 2, 187–197.
- [2] Baez, J.; Langford, L., *Higher-dimensional algebra IV: 2-Tangles*, to appear in Adv. Math, preprint available at

<http://xxx.lanl.gov/abs/math.QA/9811139> .
- [3] Brieskorn, E., *Automorphic sets and singularities*, Contemporary math., 78 (1988), 45–115.
- [4] Carter, J.S.; Jelsovsky, D.; Kamada, S.; Langford, L.; Saito, M., *Quandle cohomology and state-sum invariants of knotted curves and surfaces*, preprint at

<http://xxx.lanl.gov/abs/math.GT/9903135> .
- [5] Carter, J.S.; Kauffman, L.H.; Saito, M., *Structures and diagrammatics of four dimensional topological lattice field theories*, to appear in Advances in Math.

- [6] Carter, J.S.; Rieger, J.H.; Saito, M., *A combinatorial description of knotted surfaces and their isotopies*, Advances in Mathematics, 127, No. 1, April 15 (1997), 1–51.
- [7] Carter, J.S.; Saito, M., *Knotted surfaces and their diagrams*, the American Mathematical Society, 1998.
- [8] Carter, J.S.; Saito, M., *Surfaces in 3-Space that do not lift to embedding in 4-Space*, in Banach Center Proceedings, 42 (1998) Knot theory, 29–47.
- [9] Carter, J.S.; Saito, M., *On formulations and solutions of simplex equations*, Internat. J. Modern Phys. A 11 (1996), no. 24, 4453–4463.
- [10] Carter, J.S.; Saito, M., *Some new solutions to the permutohedron equation*. Proceedings of the Conference on Quantum Topology (Manhattan, KS, 1993), 51–65, World Sci. Publishing, River Edge, NJ, 1994.
- [11] Carter, J.S.; Saito, M., *Canceling branch points on the projections of surfaces in 4-space*, Proc. AMS 116, 1, (1992) 229-237.
- [12] Dijkgraaf, R., and Witten, E., *Topological gauge theories and group cohomology*, Comm. Math. Phys. 129 (1990), 393–429.
- [13] Fenn, R.; Rourke, C., *Racks and links in codimension two*, Journal of Knot Theory and Its Ramifications Vol. 1 No. 4 (1992), 343-406.
- [14] Fenn, R.; Rourke, C.; Sanderson, B., *Trunks and classifying spaces*, Appl. Categ. Structures 3 (1995), no. 4, 321–356.
- [15] Fenn, R.; Rourke, C.; Sanderson, B., *James bundles and applications*, preprint found at

<http://www.maths.warwick.ac.uk/~bjs/> .
- [16] Flower, Jean, *Cyclic Bordism and Rack Spaces*, Ph.D. Dissertation, Warwick (1995).
- [17] Fox, R.H., *A quick trip through knot theory*, in Topology of 3-Manifolds, Ed. M.K. Fort Jr., Prentice-Hall (1962) 120–167.
- [18] Giller, C., *Towards a classical knot theory for surfaces in \mathbf{R}^4* , Illinois Journal of Mathematics 26, No. 4, (Winter 1982), 591-631.
- [19] Greene, M. T. *Some Results in Geometric Topology and Geometry*, Ph.D. Dissertation, Warwick (1997).
- [20] Hartley, R., *Identifying non-invertible knots*, Topology, 22 (1983), 137-145.
- [21] Jelsovsky, D. ; Saito, M., *Maple programs for computing quandle cohomology and cocycle knot invariants*,

<http://www.math.usf.edu/~saito/maple.html> .

- [22] Jones, V.F.R., *Hecke algebra representations of braid groups and link polynomials*, Ann. of Math., 126 (1989), 335-388.
- [23] Joyce, D., *A classifying invariant of knots, the knot quandle*, J. Pure Appl. Alg., 23, 37–65.
- [24] Kamada, S., *Surfaces in \mathbf{R}^4 of braid index three are ribbon*, Journal of Knot Theory and its Ramifications 1 (1992), 137-160.
- [25] Kamada, S., *A characterization of groups of closed orientable surfaces in 4-space*, Topology 33 (1994), 113-122.
- [26] Kamada, S., *2-dimensional braids and chart descriptions*, “Topics in Knot Theory (Erzurum, 1992),” 277–287, NATO Adv. Sci. Inst. Ser. C Math. Phys. Sci., 399, Kluwer Acad. Publ., (Dordrecht, 1993).
- [27] L. H. Kauffman, *Knots and Physics*, World Scientific, Series on knots and everything, vol. 1, 1991.
- [28] Kawauchi, A., *A survey of knot theory*, Birkhauser, 1996.
- [29] Kawauchi, A., *The invertibility problem on amphicheiral excellent knots*, Proc. Japan Acad., Ser.A, Math. Sci. (1979), 55, 399-402.
- [30] Langford, L., *2-tangles as a free braided monoidal 2-category with duals*, Ph.D. dissertation, U.C. Riverside, 1997.
- [31] Litherland, R. A., *Symmetries of twist-spun knots*, in “Knot theory and manifolds” (Vancouver, B.C., 1983), 97–107, Lecture Notes in Math., 1144, Springer, Berlin-New York, 1985.
- [32] Matveev, S., *Distributive groupoids in knot theory*, (Russian) Mat. Sb. (N.S.) 119(161) (1982), no. 1, 78–88, 160.
- [33] Murasugi, K., *Knot theory and its applications*, Translated from the 1993 Japanese original by Bohdan Kurpita. Birkhuser Boston, Inc., Boston, MA, 1996.
- [34] Neuchl, M., *Representation Theory of Hopf Categories*, to appear in Adv. in Math. under the title *Higher-dimensional algebra VI: Hopf categories*, Available at:

<http://www.mathematik.uni-muenchen.de/~neuchl> .
- [35] Turaev, V., *The Yang-Baxter equation and invariants of links*, Invent. math. 92 (1988) 527–553.
- [36] Turaev, V., “Quantum invariants of knots and 3-manifolds,” de Gruyter Studies in Mathematics, 18. Walter de Gruyter & Co., (Berlin, 1994).
- [37] Roseman, D., *Reidemeister-type moves for surfaces in four dimensional space*, in Banach Center Publications 42 (1998) Knot theory, 347–380.

- [38] Rosicki, Witold, *Some Simple Invariants of the Position of a Surface in \mathbf{R}^4* , Bull.of the Pol. Ac.of Sci. Math. 46(4), 1998, 335-344.
- [39] Rudolph, L., *Braided surfaces and Seifert ribbons for closed braids*. Comment. Math. Helv. 58 (1983), no. 1, 1–37.
- [40] Rolfsen, D., *Knots and Links*. Publish or Perish Press, (Berkley 1976).
- [41] Wakui, M., *On Dijkgraaf-Witten invariant for 3-manifolds*, Osaka J. Math. 29 (1992), 675–696.
- [42] Zeeman, E. C., *Twisting spun knots*, Trans. Amer. Math. Soc. 115 (1965) 471–495.